# MEASUREMENT OF MAGNE[illegible] SUSCEPTIBILITY ON TAILINGS CORES

## REPORT ON CORES OBTAINED FROM THE ONTARIO RESEARCH FOUNDATION LYSIMETER EXPERIMENT

TITLE:

# MEASUREMENT OF MAGNETIC SUSCEPTIBILITY ON TAILINGS CORES REPORT ON CORES OBTAINED FROM THE ONTARIO RESEARCH FOUNDATION LYSIMETER EXPERIMENT

Work on this project was conducted under the auspices of the National Uranium Tailings Program of the Canada Centre for Mineral and Energy Technology, Energy, Mines and Resources Canada

DSS File No. 15SQ.23241-4-16[illegible]84

DSS Contract Serial No. OSQ84-00103

CANMET PROJECT NO.

CANMET Scientific Authority: Mr.G.M.Ritcey

OCTOBER 1984

88pp

MAR 15 1985

MICROMEDIA

**Abstract**

Bulk susceptibility and induced magnetic remanence results are reported for 40 cores obtained from the uranium tailings lysimeter experiment at the Ontario Research Foundation. Both methods indicate a broad threefold subdivision of the tailings pile. An upper zone is characterised by an enhanced susceptibility level, which is related to enhanced concentration of both magnetite and hematite. Depletion zones, where present, are of limited areal extent and strongly developed. An intermediate zone is characterised by a mixture of large areas of reduced susceptibility that separate smaller regions of slightly enhanced susceptibility. The zones of susceptibility depletion appear to define a dendritic drainage pattern. Locally in this zone magnetite is enhanced and hematite depleted. In the lowermost zone susceptibility levels are reduced over most of the tailings bed. Only in the upper most right hand corner is there any vestige of a positive susceptibility concentration. Both magnetite and hematite are strongly depleted in this lower zone. Visually it is apparent that this lowermost depleted zone correlates to the zones of strongest "yellowcake" development.

## INTRODUCTION

Each magnetic susceptibility reading is a measure of the field temporarily generated in a sample upon application of a low d.c. field. Variations in magnetic susceptibility between specimens are a function of three parameters affecting the iron-titanium oxides contained in the specimen. The first factor is oxide mineral composition. For example, magnetite has a much higher unit volume susceptibility than hematite. The second factor is oxide mineral content. Obviously the higher the oxide mineral content, the higher the susceptibility signal. The third factor is oxide mineral grain size. Many studies have shown that given a constant mass of oxide mineral in a specimen, higher susceptibility signals are obtained with increasing grain size, while finer grain sizes give lower susceptibility values.

A variation in at least one of these parameters is required to produce susceptibility variations over a given volume of rock. An intrinsic assumption of the lysimeter samples examined in this study is the complete homogeneity of the tailings upon experiment commencement. This assumption requires that, if sampled upon initiation, all specimens should be recording the same susceptibility value within some stated experimental error. If the tailings are homogeneous there should be no significant variations in oxide mineral content, composition, or grain size. Any differences in susceptibility values observed upon completion

of the experiment then must be reflecting the effects of processes which have modified the distribution of the oxide phases during the experiment. The geological processes affecting the distribution of oxide phases fall into two main categories, either hydraulic, or chemical.

Hydraulic effects concern the physical transportation of oxide particles from their initial position to some other location of lower water flow rate. While the bed surface offers the best opportunity for the development of this effect, high volumes of water are known also to pass through the bed. In the lysimeter experiment, rain is simulated by concentrated overhead sprinklers, and at least some localised grain migration from the "sink holes" should be expected. In a more natural environment hydraulic related susceptibility reduction may arise from a reduction in the average oxide grain size produced by downstream grain attrition.

Chemical effects produce changes in the average oxide composition and grain size by the interaction of oxide particles and mineralised fluids. Both positive and negative oxide contributions would arise from the formation of new oxide species such as hematite by the dehydration of oxy-hydroxides. Negative contributions may arise from a change in composition of the magnetic oxide species, say hematite to rutile, and by a reduction in the average oxide grain size. Both of these effects could be active where magnetite is altered to the less magnetic mineral hematite.

The chemical stability of hematite relative to magnetite in a hydrous environment is a function of the eH and pH of the water. Reducing conditions prefer the formation of magnetite, while oxidising or acidic conditions prefer the generation of hematite. The deposition or hydrous transport of uranium is closely associated with the status of the iron-titanium oxides. For example, our studies in the Thelon Formation have documented the association of uraninite mineralisation with enhanced magnetite concentrations; borehole susceptibility surveys have been used to locate uranium mineralisation zones in sedimentary strata ( see the attached paper by Hafen et al 1982); many uranium deposits in the Athabasca Basin have been associated with localised concentrations of graphitic material which produced local reducing conditions.

Magnetic susceptibility measurements appear to provide a guide to the processes which have modified the distribution of magnetic oxide particles since intiation of the tailings bed. Susceptibility studies of exploration targets suggest a correlation between the presence / absence of magnetic oxides and uranium deposition. With the above in mind, it is likely that magnetic susceptibility measurements on uranium tailings can offer a rapid method of documenting ion migration pathways in large tailings piles.

## METHODOLOGY

### Sampling

Cores of tailings were extracted from 40 locations in the ORF (Ontario Reasearch Foundation) lysimeter experiment using 1.5" ABS plastic tubing (Figure 1 and Table 1). In preparation for sampling, the tubes were cut into 1 meter lengths. One end was bevelled to provide a cutting edge to cleanly penetrate the tailings. Each tube was driven into the tailings bed using a sledge hammer. In most cases the tubes with sediment infill intact could then be simply extracted. Prior to shipment all cores were sealed at both ends by drain caps, and then wrapped and sealed in plastic sheeting to prevent moisture loss.

Immediately prior to susceptibility measurement this wrapping was removed, and a 2.5 cm interval scale was marked along the side of each core. At this stage the only absolute reference point in each core was the tip of the bevelled edge of each core. Initially this point was considered the common zero depth point. After completion of the bulk susceptibility measurements each core was cut along its length into an upper 1/3rd and lower 2/3rd section. Lithological examination of the exposed core now permitted identification of the "apparent" depth of the top surface of the tailings column, and the thickness of underlying gravel bed present in each core. Using this information all of the susceptibility logs were corrected to using the upper tailings surface as the zero common depth point.

The mineralogical compositional variations of the tailings have in part been defined by using the remanence properties of the magnetic oxides. Preparation of specimens for these studies involved sub-sampling of the thicker 2/3rd core segment using one inch square plastic cubes. After extraction from the core each cube was sealed using casting resin. The application of large d.c. magnetic fields causes a permanent alignment (magnetic remanence) of magnetic domains in oxide particles. Like susceptibility magnetic remanence is dependant upon oxide content, composition and grain size. However, unlike susceptibility different d.c. field thresholds are required to effect vector alignment in magnetite and hematite grains. Therefore by measuring the magnetic remanence of a specimen after the application of incremental d.c. magnetic fields it is possible to separate the contributions to the total saturation magnetic remanence intensity caused by magnetite and hematite.

## Measurements

All susceptibility measurements were performed on a Sapphire Instruments SI-1 susceptibility bridge. Measurements were made at 2.5 cm intervals along each core. As the measurement coil is approximately 7.0 cm wide, the first measurement that could be obtained was 7.5 cm from the tip of the tube. The last measurement taken on each core was when the bulk susceptibility level dropped below 1 x10-6 emu. At the outset it was anticipated that only small differences in susceptibility level could be expected. To ensure these differences could be recognised it was thought necessary to adopt a measurement procedure where the second decimal point of susceptibility value was considered valid. To provide this degree of accuracy each level on each core was measured five times. Prior to each of the five readings the coil was zeroed. The susceptibility values quoted for each level are the logarithmic average of the five observations. (Subsequently, it was found that the observed values exhibited order of magnitude variations).

In this study 1.5 KOe was used as the threshold limit for magnetite remanences, and the difference between 1.5 KOe, and 7.5 KOe remanence values as an indicator of hematite remanences. All remanence measurements were made on a Schonstedt DSM-1 spinner magnetometer.

## RESULTS

### Susceptibility

Results of the bulk susceptibility measurement on core from the O.R.F. tailings lysimeter are presented in figures 2,3,4,5 and 6, and Table 2.

The susceptibility results are presented in the form of the difference between the log 10 (susceptibilty value *10+6) at each level and a logarithmic collection mean susceptibility value (3.78 x10-5 emu). As discussed above positive deviations represent regions of oxide enhancement, while negative deviations represent areas of oxide depletion. All values are quoted relative to the current logarithmic average value for the tailings bed. This does not necessarily represent the absolute state of oxide distribution. Some of the original iron content may have been lost in the effluent. (All zones may be partially depleted).

Figure 2 presents a normal probability plot of all the data present in Table 2. Three definite populations of susceptibility data can be identified. These are; a) leached tailings, b) unaltered tailings, and c) gravel biased readings. The reality of the fourth population identified in figure 2 is uncertain. Either this slope represents the partial overlap between the unaltered

and gravel biased populations or the slope represents the signature of the effects of oxide enrichment. As many of the results which contribute to this population come from the top surface of the cores the latter interpretation is the one presently preferred. The boundary between the leached, and unaltered tailings at approximately -0.75 serves to separate regions of oxide depletion from essentially unaltered tailings. The boundary between the unaltered and oxidised tailings at approximately +0.75 likewise identifies the regions of oxide enhancement.

The gravel biased results do not provide any meaningful information about oxide mobility in the tailings pile. Gravel which forms the base to the tailings pile has much higher per unit volume susceptibility than the tailings. Susceptibility readings on any core which penetrated into the gravel base of the lysimeter become spurious when the portion of the core containing the gravel is brought within proximity of the measuring coil. All such spurious readings are identified in Table 2 by an asterisk.

Figures 3, 4, and 5 present contour plots of susceptibility deviation values with increasing depth from the lysimeter bed surface. On all plots the contour interval is 0.5 deviation units. Regions of depletion (<-0.5) are identified by vertical lines, while regions of enhancement (>+0.5) are identifed by a stipple ornament.

General features of contour plots 3, 4, and 5 are:-

a) Plots of near surface susceptibility values show a much higher proportion of oxide enriched zones, while plots of deeper levels always contain a higher proportion of oxide depleted zones.

b) The area near the beach outlet is oxide depleted at all levels relative to the remainder of the lysimeter.

c) Some plots, for example the 7.5 cm depth level, show pronounced effects caused by the boundaries of the lysimeter box.

With increasing depth the following specific features can be recognised:-

a) -7.5 cm. This horizon is dominated by two broad susceptibility enhanced regions separated by a narrow depleted zone which extends the total length of the lysimeter. The depleted zone widens out rapidly at the beach zone. An intensely localised zone of oxide depletion is found at core 25, and extends downstream with less pronounced effect to core 23. Upstream at 31 and 35 is a small zone of localised oxide enhancement.

b) -10.0 cm. The depleted zone becomes more intense in the region of the beach. Over the remainder of the lysimeter the depleted zone becomes less intense and of wider extent. The localised negative has shifted down to core 23 and is of lower intensity.

c) -12.5 cm. The intense depleted zone near the beach extends up the bed to include the depleted zone around core 23. Three isolated zones of enhancement become defined. What was originally a continuously enhanced zone along the left side of the lysimeter (on the diagram) is now separated into two zones by a weak trough.

d) -15.0 cm. The positive areas on the left of the lysimeter become even more diminished. Also the positive region on the right of the lysimeter (as shown on the diagram) is separated by a trough into two regions. The first imprint of a dendritic drainage pattern is developed. The area around cores 23 and 25 is now a small positive zone. Whatever the feature that was causing the localised depletion in zones above 12.5 cm. does not extend below 15 cm.

e) -17.5 cm. The highs on the left of the lysimeter are diminished to the extent that there are no regions of enrichment remaining. On the right the depleted trough between the two highs becomes more pronounced. The dendritic drainage pattern is more pronounced.

f) -20.0 cm. The dendritic drainage pattern attains its most pronounced development. Small isolated enhanced zones are separated from each other by a well defined branching pattern of depleted zones. At the point of confluence of the three depleted zones, around cores 7, 27, and 26, the level of depletion as expected becomes more intense.

g) -22.5 cm. Initiation of the breakdown of the dendritic drainage pattern. Only the upper right hand corner remains as a well defined enhanced zone. All other enhanced areas become weakly defined. The depleted zone extends further across the bed.

h) -25.0 cm. and -27.5 cm. Record the migration of the depleted zone to other parts of the lysimeter.

i) -30 cm. Finally the depleted zone represents over 50% of the total area of the lysimeter. Enhanced zones where present are weakly developed and poorly constrained by the data.

In summary we can describe the lysimeter as showing the three following characteristic zones:-

a) an upper zone of oxide enrichment with intense localised depleted zones.

b) a middle zone characterised by a dendritic pattern of broad oxide depleted zones which separate local weakly enhanced areas.

c) a lower zone characterised by extensive oxide depletion.

## Magnetite and Hematite Distributions

Figures 6, 7, 8, and 9 together with Tables 3 and 4 present the results of the remanent magnetisation studies of oxide mineralogical composition. The values quoted in both Tables 3 and 4 are emu x10-3, representing respectively for magnetite the remanence intensity increase upon application of a 1.5 KOe d.c. magnetic field, and for hematite the intensity increase between the 1.5 KOe and a 7.5 KOe field. As with the susceptibility data the stipple pattern represents a zone of enhanced oxide content, while the vertical lines indicate oxide depleted zones.

Figure 6 presents a profile of the susceptibility, magnetite and hematite variations along lone 3. Significant features of this diagram are:-

a) The well defined stratification of the susceptibility plot with an enhanced zone near the surface, an unaltered zone next, and a depleted zone at the base. Note also the localised low around cores 23 and 25 that was identified above in the contour plots.

b) Both magnetite and hematite are enhanced in the near surface zone. A second discontinuous zone of enrichment is found in the magnetite values. In the hematie data this zone appears to correspond to a narrow well defined band of abnormally low hematite values.

c) Both magnetite and hematite exhibit a narrow zone of depletion near the base of the tailings pile. The hematite defined low is more continuous than the magnetite equivalent feature.

Figure 7 summarising the same three data elements (susceptibility, magnetite, and hematite) for line 6 shows many of the same features that are described above for line 3.

a) The susceptibility data generally show a simple three fold subdivision, enhanced oxidised zone on top, unaltered zone in the middle, and a depleted or leached zone at the base. On line 6 in contrast to line 3; the top surface contains a depleted zone of broad surface distribution but limited depth extent; localised enhanced zones within a much larger zone of unaltered tailings; and a much more larger depleted zone.

b) Again the magnetite data show an upper and a lower enriched zone which merge into one broad enriched zone towards the beach. On this line the magnetite enhanced zone does not extend to the surface. Again a well defined magnetite depleted zone is found at the base of the tailings pile.

c) For the most part line 6 is characterised by average hematite values. Enhancement is found only in two merging narrow near surface zones. Yet once more the base of the tailings is hematite depleted.

Figures 8 and 9 which present the susceptibility, magnetite and hematite data for respectively rows E and F confirm the features of the line 3 and line 6 data.

a) Susceptibility: an enhanced zone in a near surface position, an unalterd zone at intermediate depths, and a depleted zone at the base of the tailings bed.

b) Magnetite enrichment in the near surface and depletion at depth.

c) Hematite enrichment in the near surface, and two narrow depleted zones at depth.

Both figures 8 and 9 show a marked contrast between the left and right sides of the lysimeter box (as seen on the figures). Especially along row E these changes correlate to the positions where bed thickness rapidly changes. It is possible these features arise as from the localised flow regime being controlled by the geometry of the base of the tailings bed.

## LIMITATIONS AND RESTRICTIONS

Figure 6 shows two important aspects concerning limitations on the significance of the contour plots. First, the 40 cores sampled from the ORF lysimeter experiment are not uniformly distributed. Control on localised susceptibility variations especially for the shallower depths is more tightly constrained towards the beach area, and the centre of the lysimeter, than it is for the regions above row D. Second, significant changes in the thickness of the tailings bed limit control on susceptibility variations for the deeper levels near the beach area. And more importantly have exercised an important effect on fluid motions through the bed.

In three dimensions the tailings bed has the form of a truncated wedge. A problem with presentation of the observed data is a decision concerning what should be used as the correct reference surface. The beds do not contain any absolute horizontal surface to which all data can be correlated. We have chosen for convenience to use the top surface of the tailings bed, although we recognise that this surface may itself be sloping and undulatory. However it provides the most easily defined reference point. In future studies more exact control of this problem is required.

A related problem concerns cross-correlation of data between results from adjacent cores, where the two cores have different lengths, say L1 and L2. If both of these cores represent the same total time span then position L1/n would be equivalent to L2/n, where n would be some portion of the total time interval N. In this case an equivalent time zone in two adjacent cores would be represented by a different thickness of sediment in the two cores. Yet our adopted observation procedure used a uniform sample spacing. As in this example we have no reason to believe that the tailings thickness represents time effects - the bed was homogeneously deposited - we used the simple unit thickness approach for contouring. Again natural environments may require more sophisticated analytical procedures.

## CONCLUSIONS

A thorough rock magnetic study of 40 cores from the O.R.F. uranium tailings lysimeter has permitted recognition of the following features:

a) The observed susceptibility data define four separate log-normal populations. Three of these four populations provide information on the mobility of iron-titanium oxides through the tailings pile.

b) Using the susceptibility data together with information derived from saturation remanence studies on magnetite and hematite variations in the tailings it is possible to recognise three distinct zones in the lysimeter box.

c) The uppermost zone is defined by a preponderance of enhanced susceptibility levels. This zone is intimately associated with enhanced magnetite and hematite levels. Depleted zones are of limited areal extent, and where present are strongly developed. The main fluid migration pathway within this zone appears to be along the bed surface. Water is also transferred towards the surface by dehydration of the bed. Evaporation would cause concentration of any water contained mineral species, almost certainly leading to the deposition of oxide rich minerals. A small frozen region near holes 23 and 25 disturbed the regional susceptibility signal especially in the near surface levels.

d) The intermediate zone is characterised by a well defined dendritic drainage pattern; there are four diffuse susceptibility enhanced zones separated by troughs of reduced susceptibility.

Typically this zone also has variable magnetite content and an average to reduced hematite content. Local concentrations of magnetite can be detected.

e) The lowermost zone is defined by strongly negative susceptibility levels. This is related to a marked depletion of both magnetite and hematite along the base of the tailings bed.

Recognition of this distribution would not have been possible with the 10 initially planned cores. A limitation of our present 40 core data set is the variable distribution of the data especially in the upper half of the bed. It is important to realise that by limited sampling one could have missed a large portion of information.

Finally, it must be emphasised that this study has shown that is is possible to use magnetic susceptibility measurements to map the distribution of magnetic oxides that is produced by fluid migration through the tailings bed. This information has lead to the recognition of three zones; a) an upper one with localised run off but mainly affected by evaporative migration, b) an intermediate zone with a dendritic drainage pattern, and c) a lower zone of widespread oxide depletion this probably being the zone through which the largest volume of fluid has passed. This study has not shown how the distrubution of magnetic oxide species is related to the distribution of environmentally dangerous chemical species. This information can either be derived from earlier ORF reports on the lysimeter, or by chemical analyses of the specimens returned to CANMET.

## RECOMMENDATIONS

The study reported above shows that magnetic susceptibility and saturation remanence measurements can be used to characterise the distribution of oxide species in the artificial environment of a lysimeter box. Recently published studies of small natural lakes (for example see attached paper by Bloemendohl et al 1979) have shown that it is possible to use the same techniques, as used in this study, to characterise sedimentologically, chemically and magnetically the variations in deposition rate within a natural small lake. We strongly recommend therefore that the magnetic susceptibility and associated saturated remanence techniques be applied to the study of a natural tailings pond environment. We envisage sampling a tailings pond in a systematic grid pattern. This would avoid any errors associated with the variable data density.

We anticipate the study of a natural tailings pond will provide information on:-

a) the natural drainage and sedimentation pattern in the pond.

b) the effects of plant material where present on the tailings bed.

c) the effects of ion migration on oxide particle distribution within the tailings bed.

## Figure Captions

Figure 1

Plan of the Ontario Research Foundation lysimeter experiment showing the location of the cores examined in this study.

Figure 2

Normal probability plot of the log10 susceptibility difference values reported in Table 2.

Figures 3, 4, and 5

Contour plots of the distribution of susceptibility difference values at different levels in the lysimeter box. Contour interval is 0.5 difference units. Areas with difference values less than -0.5 are identified by the vertical line ornament, while areas with difference vales greater than +0.5 are identified by the stipple ornament.

Figures 6, 7, 8, and 9

Profiles of the susceptibility difference, magnetite and hematite variations along Lines 3, and 6, and along Rows E and F. Contour interval on the susceptibility plots is 0.5 difference units. Areas with values <-0/5 are denoted by the vertical line ornament, while areas with values >+0.5 are denoted by the stipple ornament. For the magnetite and hematite profiles the distance between two adjacent cores represents 3 x 10-3 emu. The stepple tone identifies areas of greater than 2.0 x10-3 emu, while the vertical line ornament denotes zones of less than 1 x10-3 emu.

Figure 10

Contour of the tailings bed depth as defined by the penetration of cores into sediment pile.

TABLE 1

LOCATION OF CORES

| CORE | LOCATION | CORE | LOCATION |
|---|---|---|---|
| 1 | 1.5, 1.5 | 21 | 5.0, 7.0 |
| 2 | 2.5, 2.5 | 22 | 4.0, 7.0 |
| 3 | 5.0, 2.0 | 23 | 3.0, 7.0 |
| 4 | 5.0, 3.0 | 24 | 2.0, 6.0 |
| 5 | 8.2, 1.5 | 25 | 3.0, 6.0 |
| 6 | 8.2, 2.5 | 26 | 4.0, 6.0 |
| 7 | 5.0, 5.0 | 27 | 5.0, 6.0 |
| 8 | 1.5, 8.0 | 28 | 6.0, 6.0 |
| 9 | 5.0, 9.0 | 29 | 7.0, 6.0 |
| 10 | 8.5, 8.0 | 30 | 8.0, 6.0 |
| 11 | 2.0, 9.0 | 31 | 3.0, 5.0 |
| 12 | 3.0, 9.0 | 32 | 4.0, 5.0 |
| 13 | 4.0, 9.0 | 33 | 6.0, 5.0 |
| 14 | 6.0, 9.0 | 34 | 7.0, 5.0 |
| 15 | 7.0, 9.0 | 35 | 3.0, 4.0 |
| 16 | 8.0, 9.0 | 36 | 6.0, 4.0 |
| 17 | 3.0, 8.0 | 37 | 6.0, 3.0 |
| 18 | 4.0, 8.0 | 38 | 3.0, 3.0 |
| 19 | 6.0, 8.0 | 39 | 3.0, 2.0 |
| 20 | 6.0, 7.0 | 40 | 6.0, 2.0 |

TABLE 2

SUSCEPTIBILITY DIFFERENCE VALUES

| CORE | 1 | 2 | 3 | 4 | 5 | 6 | 7 | 8 |
|---|---|---|---|---|---|---|---|---|
| DEPTH | | | | | | | | |
| 1 | +1.68 | +0.93 | +1.31 | +1.08 | +0.83 | -0.07 | -0.33 | +0.91 |
| 2 | +1.46 | +0.86 | +1.13 | +0.72 | +0.80 | -0.09 | -0.77 | +0.73 |
| 3 | +1.37 | +0.24 | +0.43 | +0.09 | +0.62 | -0.10 | -0.88 | +0.50 |
| 4 | +1.36 | +0.35 | -0.11 | -0.04 | +0.28 | -0.06 | -0.88 | +0.26 |
| 5 | +1.31 | +0.27 | -0.09 | -0.17 | +0.09 | 0.00 | -1.18 | -0.26 |
| 6 | +1.12 | +0.15 | -0.16 | -0.06 | +0.12 | +0.01 | -1.38 | -0.88 |
| 7 | +1.05 | -0.16 | -0.20 | +0.11 | +0.11 | +0.29 | -1.32 | -1.02 |
| 8 | +1.40 | -0.23 | +0.14 | +0.27 | -0.09 | +0.71 | -1.13 | +0.68 |
| 9 | +1.66 | +0.09 | +0.32 | +0.03 | -0.93 | +0.70 | -1.08 | |
| 10 | +1.43 | +0.00 | +0.16 | -0.43 | -0.21 | +0.07 | -1.25 | |
| 11 | +0.87 | -0.35 | -0.23 | +0.19 | | -0.50 | -1.54 | |
| 12 | +0.02 | -0.54 | -0.38 | | | -0.57 | -1.46 | |
| 13 | -0.02 | -0.76 | -1.26 | | | -0.25 | -1.00 | |
| 14 | | -0.59 | | | | -0.56 | -0.45 | |
| 15 | | -0.80 | | | | | +1.49 | |
| 16 | | -0.86 | | | | | | |
| 17 | | +0.30 | | | | | | |
| 18 | | +2.47 | | | | | | |

NOTE: All values are in log 10 (x10-5) emu. Each quoted value is the difference between each spot reading and the average for all measurements.

TABLE 2 (CONTD)

SUSCEPTIBILITY DIFFERENCE VALUES

| CORE | 9 | 10 | 11 | 12 | 13 | 14 | 15 | 16 |
|---|---|---|---|---|---|---|---|---|
| DEPTH | | | | | | | | |
| 1 | -0.15 | +0.45 | +0.51 | -0.77 | -0.87 | +0.68* | +0.37* | -0.15 |
| 2 | +0.23* | +0.37 | +0.14 | -0.88 | -1.23 | +4.80* | +4.47* | +1.05* |
| 3 | +0.94* | +0.20 | -0.48 | -0.99 | -1.37 | +7.80* | +8.35* | +4.16* |
| 4 | +4.69* | -0.15 | +0.05 | -0.26 | -0.32 | +10.23* | +10.80* | +7.39* |
| 5 | +8.62* | -0.54 | +4.02* | +3.76* | +2.97 | | | +9.71* |
| 6 | +11.05* | -0.92 | +7.84* | +7.63* | +7.78* | | | |
| 7 | | -0.87 | +8.80* | +9.71* | +10.60* | | | |
| 8 | | -0.73 | | +10.16* | +12.01* | | | |
| 9 | | -0.80 | | | | | | |
| 10 | | -0.88 | | | | | | |
| 11 | | +0.57 | | | | | | |
| 12 | | +2.22* | | | | | | |
| 13 | | +1.52* | | | | | | |

TABLE 2 (CONTD)

SUSCEPTIBILITY DIFFERENCE VALUES

| CORE | 17 | 18 | 19 | 20 | 21 | 22 | 23 | 24 |
|---|---|---|---|---|---|---|---|---|
| DEPTH | | | | | | | | |
| 1 | +1.08 | +0.65 | -0.82 | -0.96 | +0.34 | +0.79 | -0.42 | +1.10 |
| 2 | +0.24 | -0.01 | -0.86 | +0.07 | +0.20 | +0.62 | -0.68 | +0.74 |
| 3 | -0.43 | -0.61 | -0.81 | +0.19 | -0.33 | -0.04 | -1.46 | +0.11 |
| 4 | -0.61 | -0.63 | -0.74 | -0.29 | -0.63 | -0.83 | -1.89 | -0.35 |
| 5 | -0.66 | -0.36 | -0.64 | -0.77 | -0.69 | -1.00 | -1.74 | -0.95 |
| 6 | -0.86 | -0.46 | -0.70 | -0.56 | -0.44 | -0.87 | -1.18 | -1.03 |
| 7 | -0.97 | -0.57 | -0.82 | -0.32 | -0.52 | -0.74 | -1.06 | -1.12 |
| 8 | -0.86 | -0.51 | -0.91 | -0.41 | -0.53 | -0.83 | -1.05 | -0.69 |
| 9 | -0.80 | +0.09 | -0.83 | -0.88 | +0.59 | -0.61 | -1.06 | -0.46 |
| 10 | +0.19 | +2.35* | -0.80 | -0.64 | | -0.36 | -0.90 | -0.51 |
| 11 | | | -0.02 | +2.43* | | +0.81 | -0.49 | -0.81 |
| 12 | | | +2.11 | | | | +0.79 | -1.09 |
| 13 | | | | | | | | -0.15 |
| 14 | | | | | | | | +2.55* |

TABLE 2 (CONTD)

SUSCEPTIBILITY DIFFERENCE VALUES

| CORE | 25 | 26 | 27 | 28 | 29 | 30 | 31 | 32 |
|---|---|---|---|---|---|---|---|---|
| DEPTH | | | | | | | | |
| 1 | -0.79 | +0.87 | +1.42 | +0.15 | +0.85 | +0.71 | +2.04 | +0.72 |
| 2 | +0.72 | +0.34 | +1.12 | +0.34 | +0.76 | +0.67 | +1.40 | +0.30 |
| 3 | +0.99 | -0.16 | +0.87 | +0.22 | +0.56 | +0.37 | +0.82 | -0.12 |
| 4 | +0.66 | -0.57 | +0.64 | +0.08 | +0.32 | +0.03 | +0.30 | -0.12 |
| 5 | +0.85 | -0.79 | +0.21 | +0.04 | +0.17 | -0.19 | +0.05 | -0.15 |
| 6 | +0.90 | -0.87 | -0.36 | +0.04 | +0.26 | -0.15 | -0.24 | -0.56 |
| 7 | +0.47 | -0.62 | -0.05 | -0.03 | +0.18 | -0.19 | -0.62 | -0.68 |
| 8 | -0.30 | -0.52 | +2.18* | -0.43 | +0.07 | -0.33 | -0.88 | -0.57 |
| 9 | -0.93 | -0.62 | | -0.60 | -0.07 | -0.24 | -1.13 | -0.32 |
| 10 | -1.22 | -0.72 | | -0.86 | -0.20 | -0.14 | -1.07 | -0.61 |
| 11 | -1.36 | -0.72 | | -0.96 | | -0.04 | -1.33 | -1.04 |
| 12 | -1.31 | -0.10 | | -0.24 | | -0.56 | -1.75 | -1.08 |
| 13 | -0.07 | +0.87 | | | | | -0.96 | -0.92 |
| 14 | | | | | | | +1.86* | -1.53 |

TABLE 2 (CONTD)

SUSCEPTIBILITY DIFFERENCE VALUES

| CORE | 33 | 34 | 35 | 36 | 37 | 38 | 39 | 40 |
|---|---|---|---|---|---|---|---|---|
| DEPTH | | | | | | | | |
| 1 | -0.48 | +0.78 | +0.76 | -0.74 | -0.74 | +0.95 | +0.99 | -0.04 |
| 2 | +0.15 | +0.96 | +0.51 | -0.37 | +0.08 | +0.84 | +1.64 | +0.20 |
| 3 | +0.35 | +0.85 | +0.27 | -0.09 | +0.59 | +0.65 | +1.91 | +0.39 |
| 4 | +0.19 | +0.54 | -0.04 | -0.04 | +0.44 | +0.52 | +1.63 | +0.48 |
| 5 | -0.16 | +0.15 | -0.56 | -0.01 | +0.34 | +0.44 | +1.63 | +0.47 |
| 6 | -0.20 | -0.55 | -0.27 | +0.07 | +0.20 | +0.42 | +1.53 | +0.50 |
| 7 | +0.08 | | +0.15 | -0.12 | +0.47 | +0.35 | +1.12 | +0.38 |
| 8 | +0.69 | | +0.24 | -0.36 | +0.74 | +0.01 | +0.28 | +0.27 |
| 9 | +0.62 | | +0.01 | -0.33 | +0.81 | +0.13 | -0.17 | +0.58 |
| 10 | +0.11 | | +0.27 | -0.06 | +0.62 | -0.14 | -0.76 | +0.67 |
| 11 | -0.23 | | +0.72 | -0.04 | +0.12 | -0.42 | -1.19 | +0.52 |
| 12 | -0.47 | | +1.11 | -0.64 | | -0.56 | -1.54 | -0.01 |
| 13 | -0.64 | | +2.20 | -0.45 | | -0.62 | | -0.36 |
| 14 | | | | -0.71 | | -1.24 | | -0.53 |
| 15 | | | | -1.22 | | | | -0.58 |

TABLE 3

MAGNETITE SIGNAL

| CORE | 7 | 12 | 14 | 17 | 19 | 20 | 23 | 24 |
|---|---|---|---|---|---|---|---|---|
| DEPTH | | | | | | | | |
| 1 | 2.00 | 2.37 | 1.54 | 3.21 | 1.42 | 1.07 | 1.79 | 2.54 |
| 2 | 1.38 | 4.32 | 1.70 | 3.31 | 1.46 | 1.51 | 2.40 | 2.90 |
| 3 | 3.18 | 1.86 | 3.36 | 1.96 | 3.05 | 2.06 | 1.65 | 1.56 |
| 4 | 1.80 | 1.60 | 1.92 | 3.03 | 1.45 | 3.15 | 1.40 | 2.45 |
| 5 | 1.75 | 1.06 | | 1.05 | 1.60 | 1.96 | 1.66 | 1.71 |
| 6 | 0.77 | 2.23 | | 2.08 | 1.47 | 1.77 | 1.30 | 1.52 |
| 7 | 0.53 | 1.36 | | 1.24 | 2.16 | 1.39 | 1.18 | 1.35 |
| 8 | 0.94 | 7.40 | | 1.47 | 1.03 | 1.92 | 1.93 | 1.29 |
| 9 | 1.10 | | | 1.75 | 1.43 | 2.01 | 1.23 | 0.86 |
| 10 | 1.69 | | | 0.72 | 1.16 | 1.30 | 1.37 | 1.92 |
| 11 | 1.57 | | | 0.97 | 1.34 | 1.11 | 2.53 | 2.72 |
| 12 | 1.18 | | | 1.05 | 0.75 | 0.76 | 1.64 | 1.52 |
| 13 | 1.19 | | | | 0.82 | 0.83 | 2.23 | 1.78 |
| 14 | 1.35 | | | | 1.12 | | 1.28 | 1.11 |
| 15 | 1.33 | | | | | | | 0.95 |
| 16 | 0.85 | | | | | | | 1.26 |
| 17 | 1.25 | | | | | | | |

NOTE: all values given in 10-3 emu. represent the remanence intensity increase after the application of an inducing field of 1500 Oe.

TABLE 3 (CONTD)

MAGNETITE SIGNAL

| CORE | 25 | 26 | 27 | 28 | 29 | 30 | 31 | 32 |
|---|---|---|---|---|---|---|---|---|
| DEPTH | | | | | | | | |
| 1 | 3.24 | 0.97 | 2.18 | 1.43 | 2.40 | 2.19 | 3.04 | 1.98 |
| 2 | 2.43 | 2.54 | 3.06 | 1.87 | 1.73 | 1.78 | 3.72 | 3.06 |
| 3 | 1.77 | 1.45 | 3.00 | 2.42 | 2.62 | 2.18 | 1.80 | 1.69 |
| 4 | 2.91 | 1.17 | 1.76 | 2.06 | 2.87 | 2.43 | 2.42 | 2.81 |
| 5 | 5.10 | 2.17 | 1.67 | 2.62 | 1.72 | 2.53 | 1.66 | 1.21 |
| 6 | 3.90 | 1.22 | 2.87 | 2.17 | 1.69 | 1.25 | 1.66 | 1.49 |
| 7 | 2.12 | 1.49 | 1.60 | 2.32 | 3.00 | 2.22 | 1.25 | 1.64 |
| 8 | 1.79 | 2.26 | 1.51 | 2.46 | 1.98 | 1.16 | 1.40 | 1.77 |
| 9 | 2.02 | 1.36 | 0.88 | 1.69 | 1.50 | 1.94 | 0.87 | 1.64 |
| 10 | 1.69 | 3.16 | 3.06 | 1.23 | 1.43 | 1.56 | 1.66 | 2.11 |
| 11 | 1.08 | 1.06 | | 1.04 | 1.72 | 1.31 | 1.56 | 1.74 |
| 12 | 0.90 | 1.30 | | 1.19 | 2.04 | 1.23 | 1.10 | 1.09 |
| 13 | 0.83 | 1.80 | | 0.79 | | 1.08 | 0.75 | 1.02 |
| 14 | 1.96 | 4.67 | | 0.81 | | 1.26 | 0.94 | 1.47 |
| 15 | | 1.52 | | | | | 1.85 | 1.24 |
| 16 | | | | | | | | 0.51 |

TABLE 3 (CONTD)

MAGNETITE SIGNAL

| CORE | 33 | 34 | 35 | 36 | 37 | 38 | 39 | 40 |
|---|---|---|---|---|---|---|---|---|
| DEPTH | | | | | | | | |
| 1 | 1.50 | 4.21 | 1.22 | 1.11 | 1.55 | 1.77 | 0.60 | 1.17 |
| 2 | 2.11 | 4.21 | 2.60 | 1.60 | 1.28 | 2.63 | 1.31 | 1.32 |
| 3 | 1.94 | 2.42 | 2.20 | 1.46 | 1.49 | 2.29 | 2.64 | 1.24 |
| 4 | 2.82 | 2.73 | 2.43 | 2.49 | 1.62 | 1.54 | 1.65 | 1.96 |
| 5 | 2.46 | 2.58 | 1.82 | 1.85 | 2.13 | 3.04 | 3.27 | 1.65 |
| 6 | 1.79 | 2.05 | 1.77 | 2.26 | 2.40 | 1.91 | 2.76 | 2.58 |
| 7 | 1.57 | 1.73 | 1.09 | 3.04 | 1.92 | 1.72 | 2.31 | 2.35 |
| 8 | 2.06 | 1.14 | 2.83 | 1.88 | 1.27 | 1.99 | 2.54 | 1.93 |
| 9 | 1.60 | | 3.76 | 1.64 | 1.42 | 1.55 | 1.74 | 2.17 |
| 10 | 2.47 | | 1.43 | 1.36 | 1.78 | 1.30 | 1.05 | 1.53 |
| 11 | 2.25 | | 1.76 | 1.55 | 2.08 | 3.19 | 1.85 | 2.49 |
| 12 | 1.40 | | 5.05 | 2.67 | 2.49 | 1.26 | 2.22 | 1.81 |
| 13 | 1.31 | | 4.48 | 1.22 | 1.70 | 1.72 | 0.82 | 2.17 |
| 14 | 1.22 | | 3.30 | 0.96 | | 2.14 | 0.68 | 1.13 |
| 15 | 1.86 | | 3.63 | 0.97 | | 0.97 | | 1.56 |
| 16 | | | | 0.90 | | | | 1.36 |
| 17 | | | | 1.04 | | | | 1.09 |

TABLE 4

HEMATITE SIGNAL

| CORE | 7 | 12 | 14 | 17 | 19 | 20 | 23 | 24 |
|---|---|---|---|---|---|---|---|---|
| DEPTH | | | | | | | | |
| 1 | 2.29 | 2.58 | 2.57 | 3.93 | 2.14 | 1.44 | 2.44 | 3.06 |
| 2 | 1.75 | 4.64 | 2.27 | 3.41 | 1.69 | 1.49 | 2.48 | 3.60 |
| 3 | 3.51 | 2.10 | 3.61 | 2.03 | 3.55 | 2.47 | 1.75 | 1.57 |
| 4 | 1.69 | 1.66 | 1.84 | 1.98 | 1.43 | 3.62 | 1.63 | 1.47 |
| 5 | 1.24 | 0.98 | | 0.81 | 1.33 | 1.86 | 1.67 | 1.47 |
| 6 | 0.52 | 2.43 | | 1.87 | 1.37 | 1.46 | 1.19 | 1.32 |
| 7 | 0.38 | 1.31 | | 1.29 | 1.80 | 1.28 | 1.12 | 1.27 |
| 8 | 0.55 | 1.55 | | 1.02 | 1.02 | 1.28 | 1.85 | 1.27 |
| 9 | 0.60 | | | 1.78 | 1.24 | 1.57 | 1.12 | 0.89 |
| 10 | 0.77 | | | 0.62 | 1.06 | 1.21 | 1.20 | 1.05 |
| 11 | 1.02 | | | 1.45 | 1.42 | 1.19 | 1.78 | 1.69 |
| 12 | 0.75 | | | 0.88 | 0.63 | 0.97 | 1.41 | 1.55 |
| 13 | 1.64 | | | | 0.97 | 0.80 | 1.75 | 1.27 |
| 14 | 1.47 | | | | 1.27 | | 1.08 | 1.54 |
| 15 | 1.26 | | | | | | | 0.59 |
| 16 | 0.80 | | | | | | | 1.27 |
| 17 | 1.33 | | | | | | | |

NOTE: All values quoted in 10-3 emu. represent the remanence intensity difference in each specimen after the application of inducing fields of 1.5 and 7.5 KOe.

TABLE 4 (CONTD)

HEMATITE SIGNAL

| CORE | 25 | 26 | 27 | 28 | 29 | 30 | 31 | 32 |
|---|---|---|---|---|---|---|---|---|
| DEPTH | | | | | | | | |
| 1 | 2.88 | 1.21 | 2.95 | 1.72 | 2.57 | 2.46 | 2.13 | 2.03 |
| 2 | 2.52 | 2.94 | 3.34 | 2.24 | 1.87 | 2.04 | 3.17 | 3.37 |
| 3 | 1.41 | 1.66 | 2.52 | 2.31 | 2.05 | 1.83 | 1.42 | 1.82 |
| 4 | 1.52 | 0.71 | 1.55 | 1.94 | 2.52 | 1.59 | 1.86 | 2.15 |
| 5 | 2.16 | 1.64 | 1.45 | 2.30 | 1.07 | 2.10 | 1.52 | 0.76 |
| 6 | 3.30 | 1.05 | 2.34 | 1.76 | 1.31 | 0.99 | 1.32 | 1.47 |
| 7 | 1.35 | 1.20 | 1.23 | 1.47 | 2.21 | 1.71 | 0.97 | 1.41 |
| 8 | 1.05 | 1.84 | 1.49 | 1.40 | 1.28 | 1.04 | 1.04 | 1.39 |
| 9 | 0.77 | 1.13 | 0.92 | 1.71 | 1.21 | 1.43 | 0.90 | 1.60 |
| 10 | 1.18 | 1.45 | 1.04 | 1.25 | 1.40 | 1.57 | 1.34 | 0.66 |
| 11 | 1.29 | 0.98 | | 0.99 | 1.47 | 1.61 | 1.27 | 0.95 |
| 12 | 1.11 | 1.30 | | 1.38 | 1.45 | 1.11 | 1.45 | 1.00 |
| 13 | 0.72 | 1.20 | | 1.04 | | 1.35 | 1.08 | 1.92 |
| 14 | 1.27 | 1.93 | | 0.69 | | 1.62 | 0.90 | 1.28 |
| 15 | | 1.04 | | | | | 0.88 | 1.20 |
| 16 | | | | | | | | 0.55 |

TABLE 4 (CONTD)

HEMATITE SIGNAL

| CORE | 33 | 34 | 35 | 36 | 37 | 38 | 39 | 40 |
|---|---|---|---|---|---|---|---|---|
| DEPTH | | | | | | | | |
| 1 | 1.65 | 2.60 | 0.69 | 1.41 | 1.47 | 2.17 | 0.73 | 1.55 |
| 2 | 2.07 | 2.52 | 1.82 | 1.96 | 1.40 | 2.76 | 1.58 | 1.61 |
| 3 | 1.88 | 2.19 | 1.62 | 1.64 | 1.85 | 2.60 | 2.66 | 1.61 |
| 4 | 2.32 | 1.99 | 1.67 | 2.75 | 1.86 | 1.50 | 1.94 | 2.89 |
| 5 | 1.50 | 1.95 | 1.34 | 1.63 | 2.24 | 1.38 | 1.58 | 1.72 |
| 6 | 1.41 | 1.65 | 1.38 | 1.42 | 1.59 | 1.60 | 1.61 | 1.65 |
| 7 | 1.19 | 1.41 | 1.03 | 1.55 | 1.29 | 1.18 | 1.94 | 1.66 |
| 8 | 1.31 | 1.04 | 1.24 | 1.52 | 1.01 | 1.54 | 1.41 | 1.63 |
| 9 | 1.50 | | 1.22 | 1.22 | 1.30 | 1.13 | 1.09 | 1.81 |
| 10 | 1.96 | | 0.72 | 1.12 | 2.08 | 0.79 | 0.93 | 1.40 |
| 11 | 1.07 | | 1.46 | 1.56 | 1.39 | 1.34 | 1.31 | 2.67 |
| 12 | 1.35 | | 2.00 | 1.90 | 1.45 | 1.11 | 1.02 | 1.53 |
| 13 | 1.25 | | 1.28 | 1.09 | 1.52 | 1.43 | 0.83 | 1.33 |
| 14 | 1.05 | | 0.45 | 0.96 | | 1.59 | 0.83 | 1.22 |
| 15 | 1.48 | | 1.78 | 0.67 | | 1.16 | | 1.02 |
| 16 | | | | 1.09 | | 0.76 | | 1.37 |
| 17 | | | | 1.26 | | | | 1.14 |

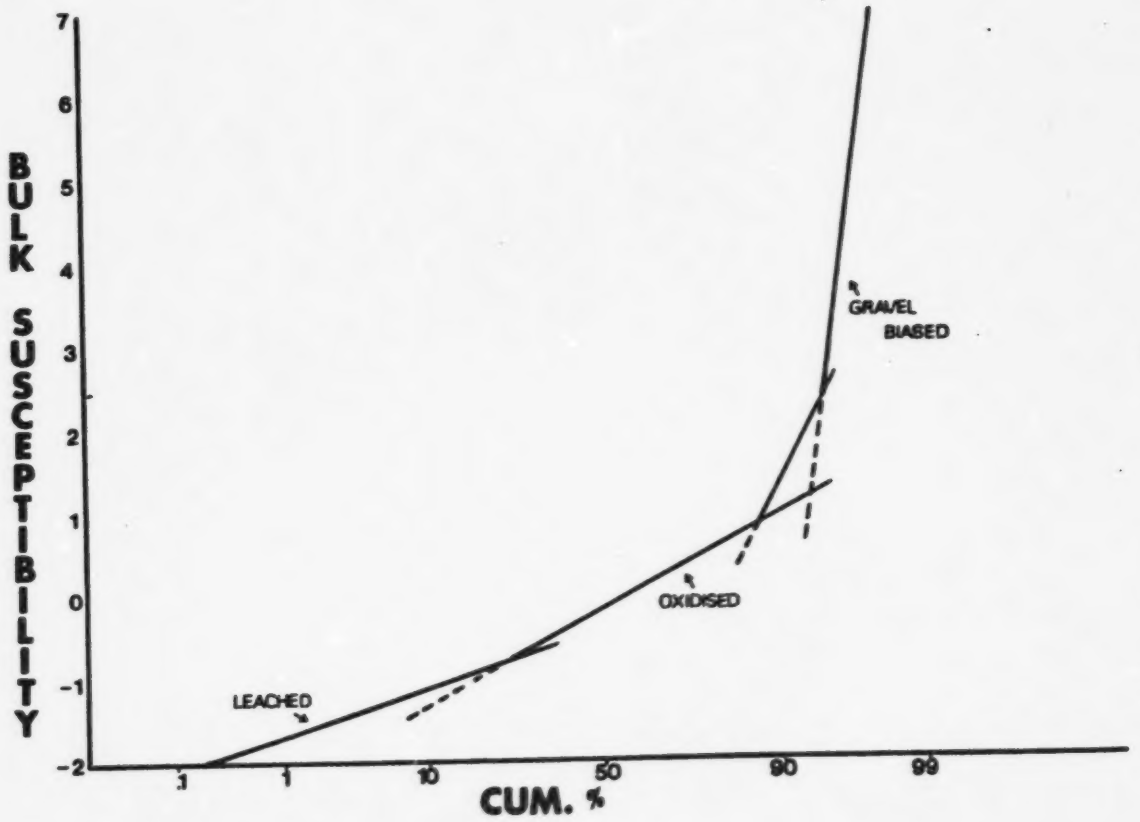
BULK SUSCEPTIBILITY
7
6
5
4
3
2
1
0
-1
-2
.1
1
10
50
90
99
CUM. %
LEACHED
OXIDISED
GRAVEL
BIASED

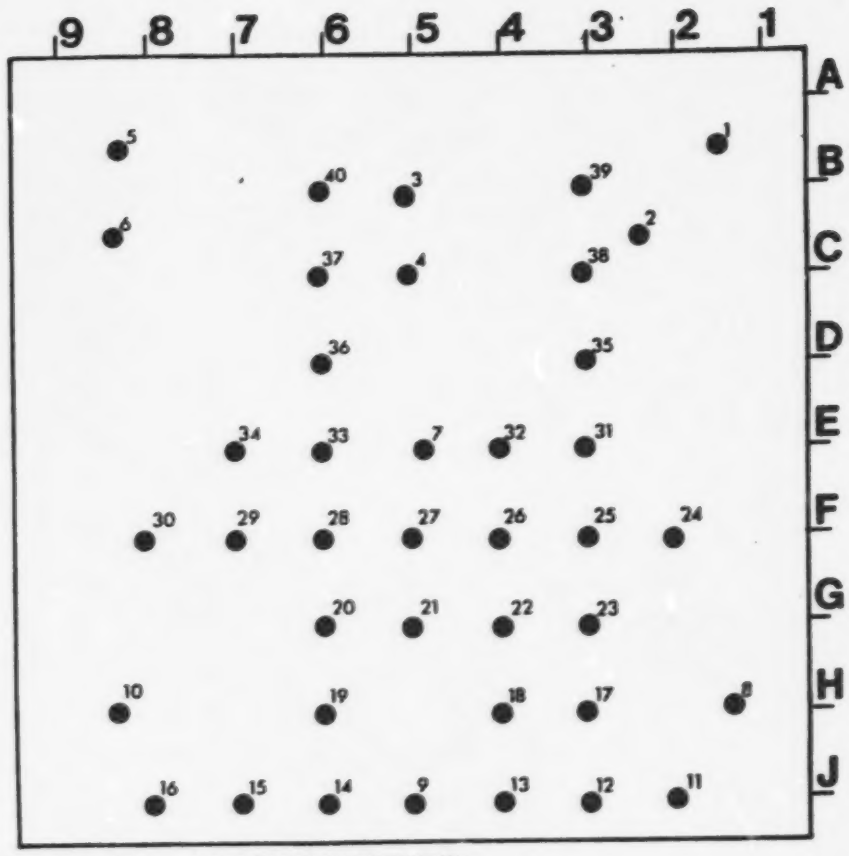


ORF LYSIMETER

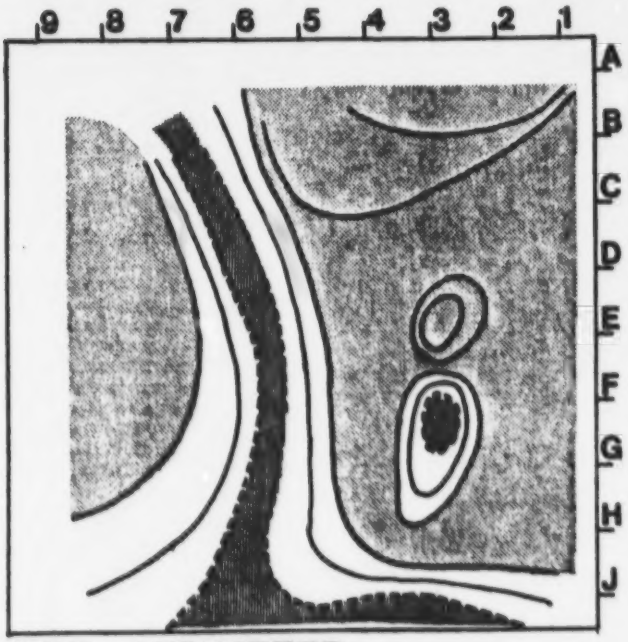


ORF LYSIMETER DEPTH (CM) : 7.5
SUSCEPTIBILITY CONTOUR INTERVAL : 0.5
WATER FLOW : ↓

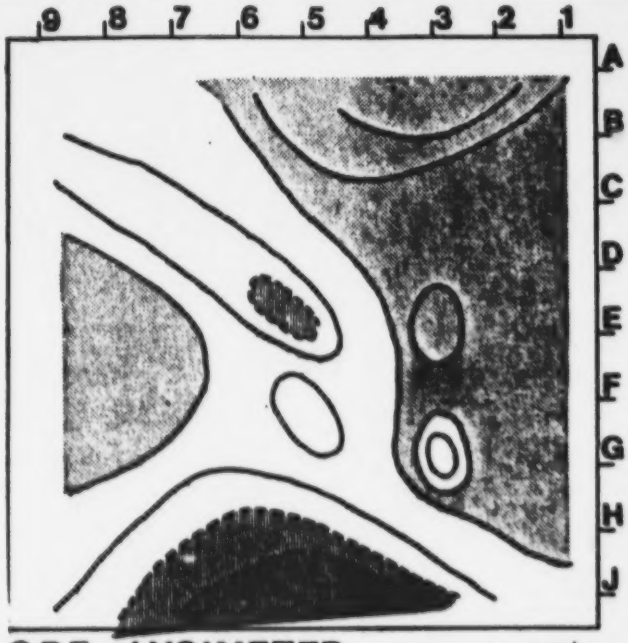


ORF LYSIMETER DEPTH (CM) : 10.0
SUSCEPTIBILITY CONTOUR INTERVAL : 0.5
WATER FLOW : ↓

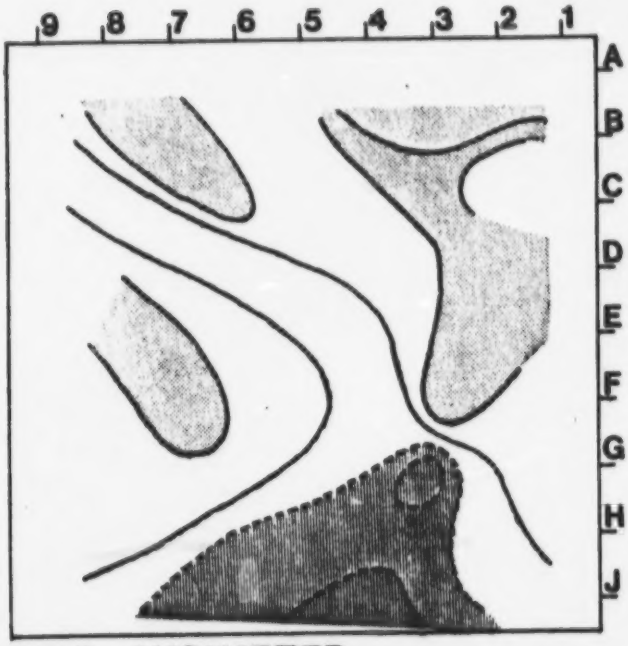


ORF LYSIMETER DEPTH (CM) : 12.5
SUSCEPTIBILITY CONTOUR INTERVAL : 0.5
WATER FLOW : ↓

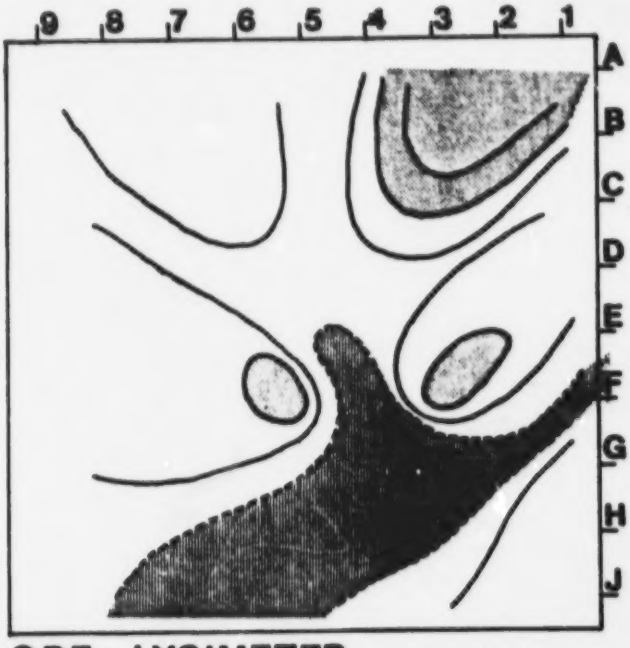


ORF LYSIMETER DEPTH (CM) : 15.0
SUSCEPTIBILITY CONTOUR INTERVAL : 0.5
WATER FLOW : ↓

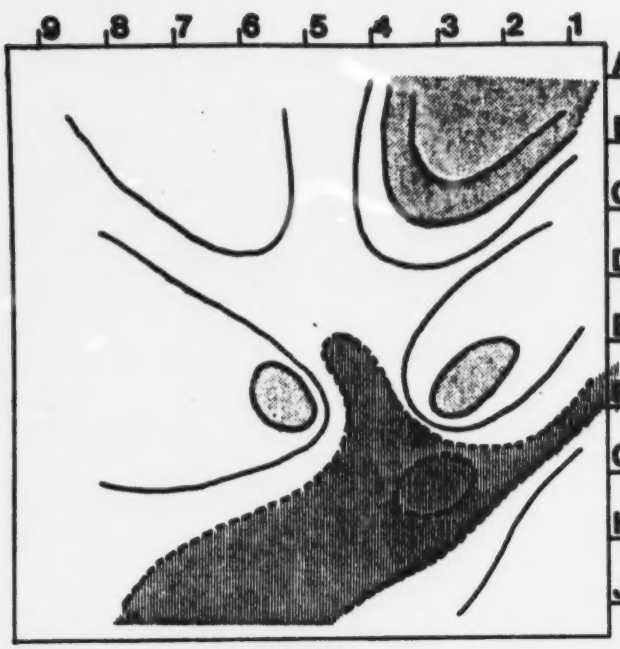


ORF LYSIMETER DEPTH (CM) : 15.0
SUSCEPTIBILITY CONTOUR INTERVAL : 0.5
WATER FLOW : ↓

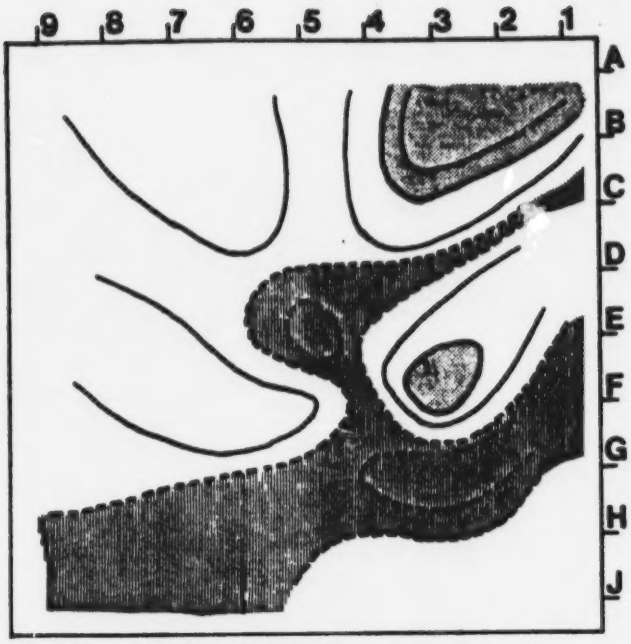


ORF LYSIMETER DEPTH (CM) : 17.5
SUSCEPTIBILITY CONTOUR INTERVAL : 0.5
WATER FLOW : ↓

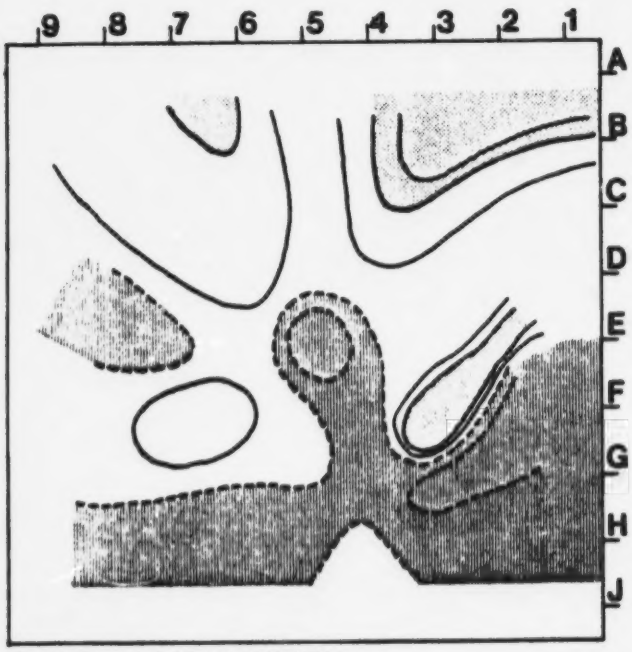


ORF LYSIMETER DEPTH (CM) : 20.0
SUSCEPTIBILITY CONTOUR INTERVAL : 0.5
WATER FLOW : ↓

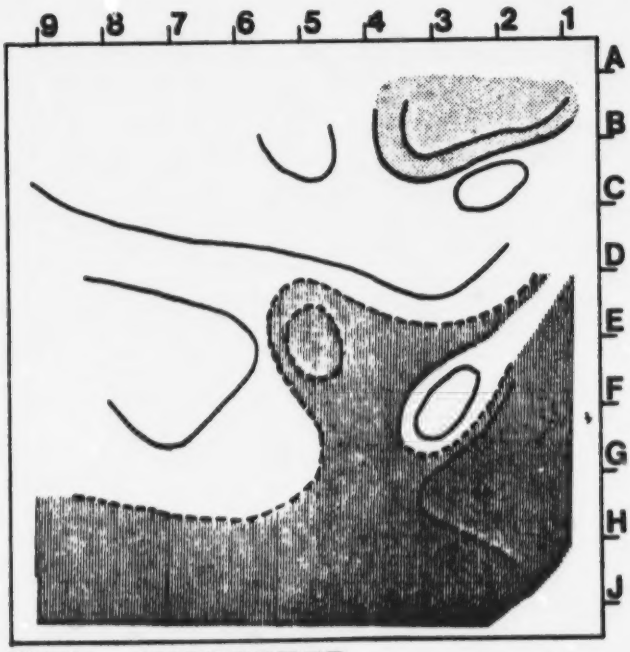


ORF LYSIMETER DEPTH (CM) : 22.5
SUSCEPTIBILITY CONTOUR INTERVAL : 0.5
WATER FLOW : ↓

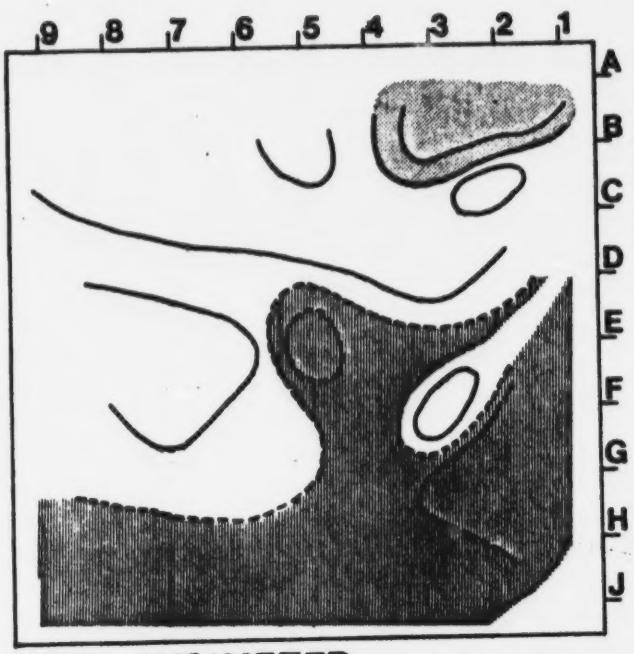


ORF LYSIMETER DEPTH (CM) : 22.5
SUSCEPTIBILITY CONTOUR INTERVAL : 0.5
WATER FLOW : ↓

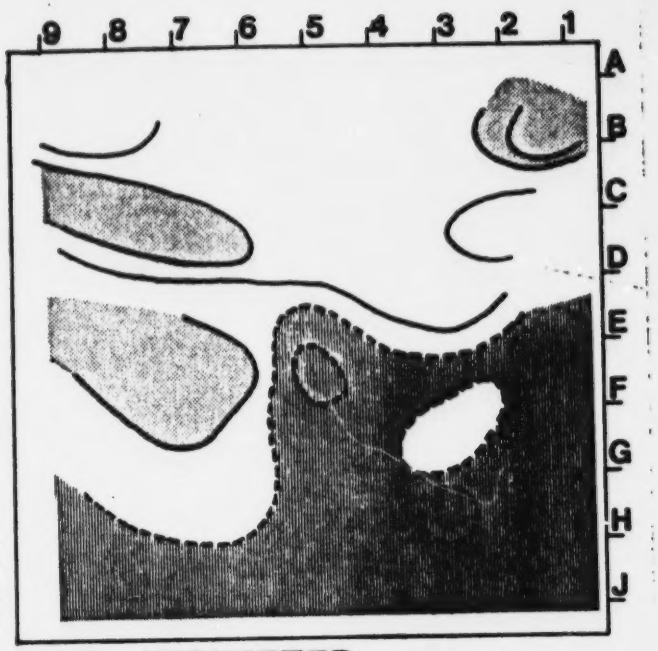


ORF LYSIMETER DEPTH (CM) : 25.0
SUSCEPTIBILITY CONTOUR INTERVAL : 0.5
WATER FLOW : ↓

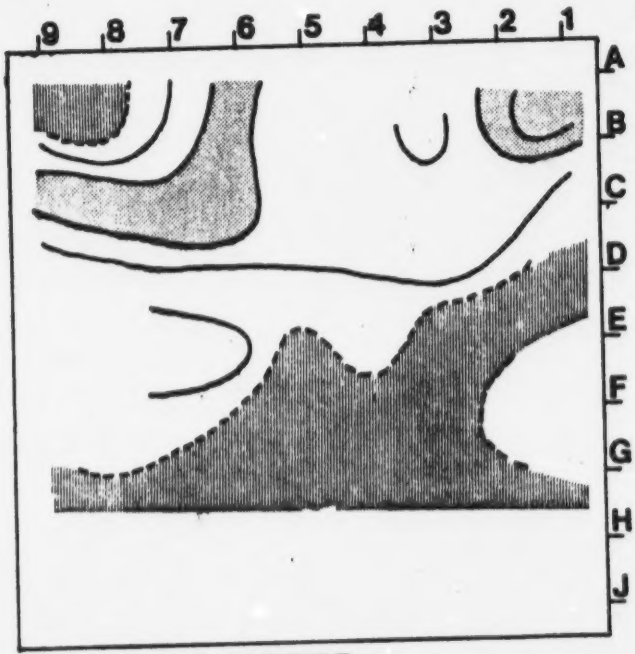


ORF LYSIMETER DEPTH (CM) : 27.5
SUSCEPTIBILITY CONTOUR INTERVAL : 0.5
WATER FLOW : ↓

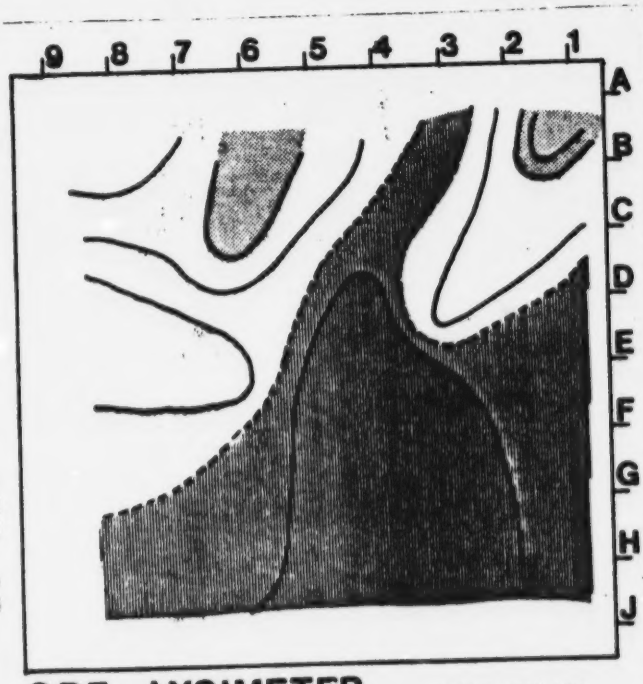


ORF LYSIMETER DEPTH (CM) : 30.0
SUSCEPTIBILITY CONTOUR INTERVAL : 0.5
WATER FLOW : ↓

# LINE 3

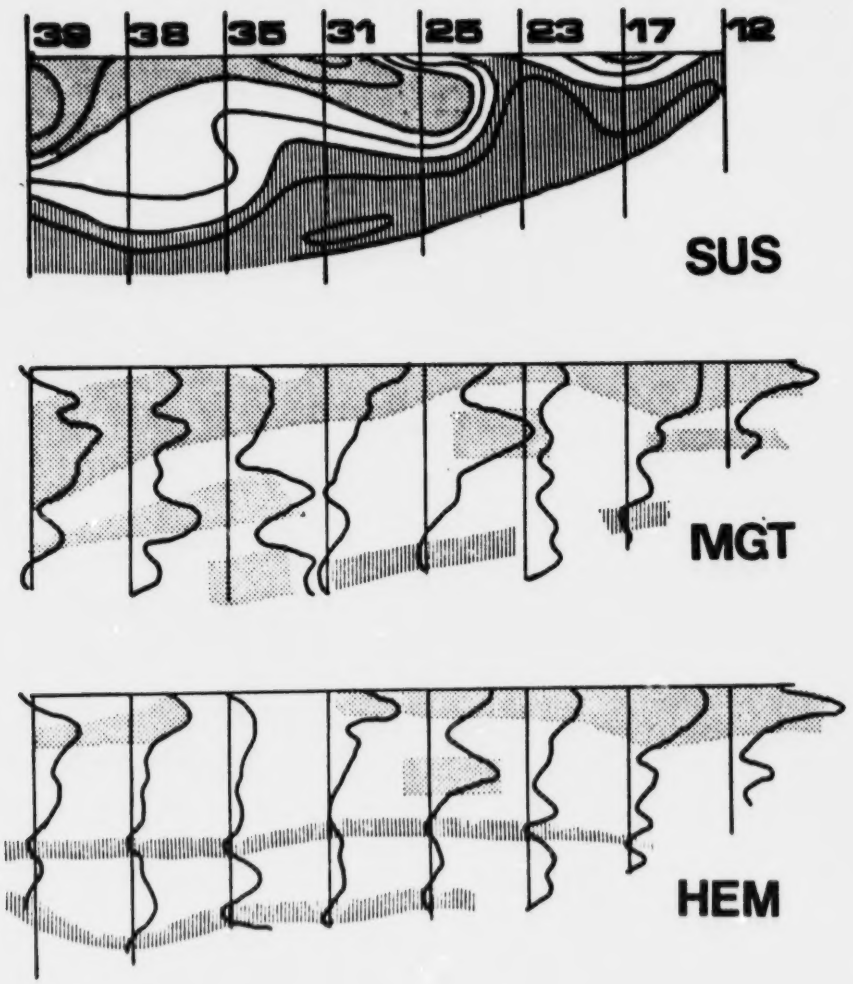

## LINE 6

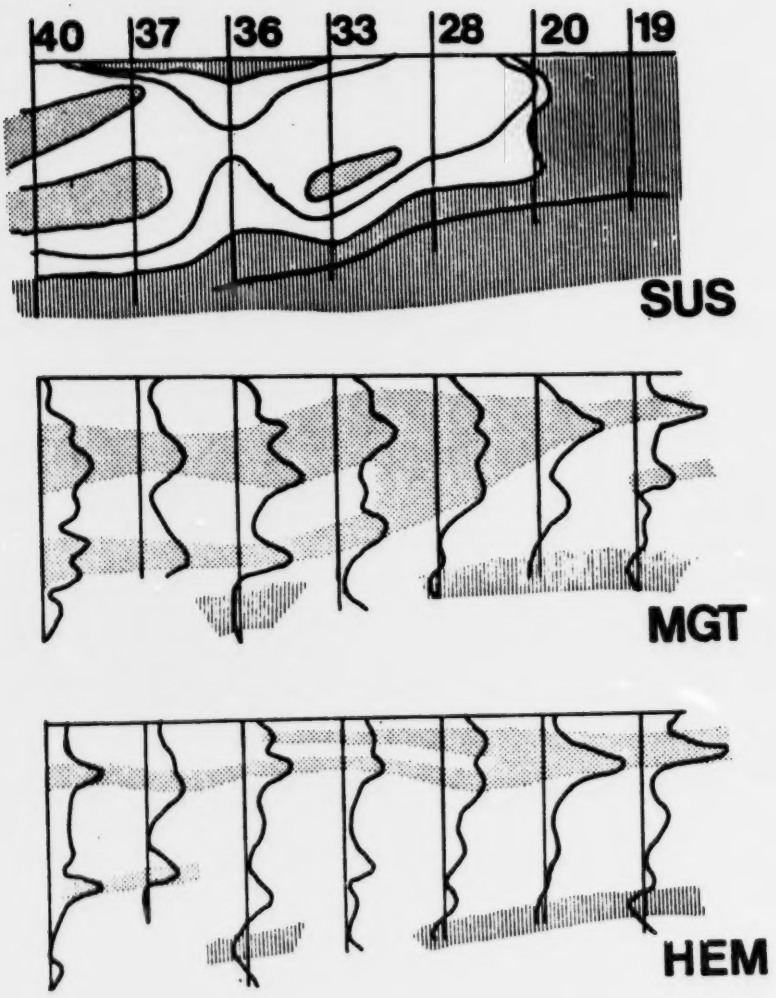

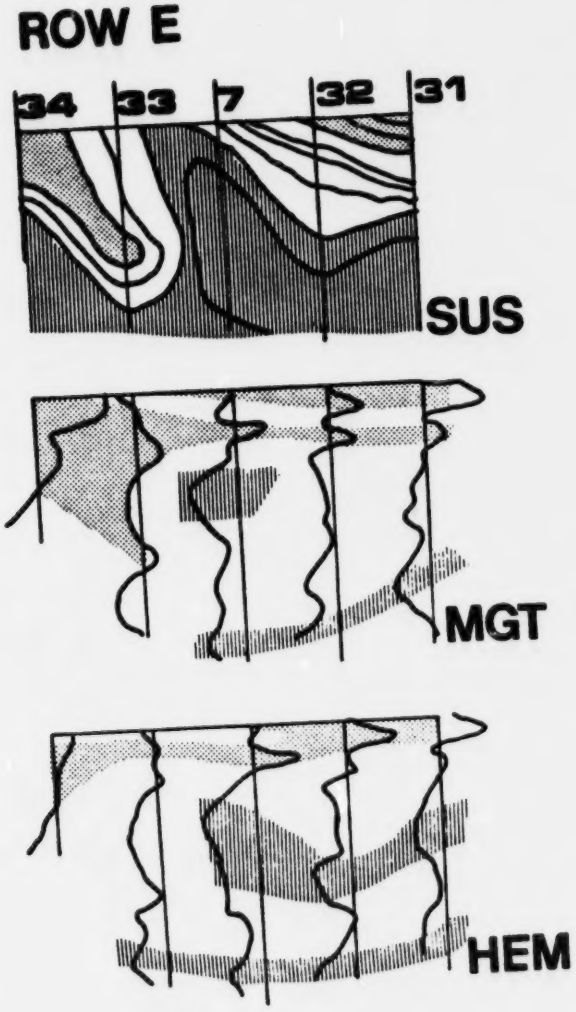
ROW E
34
33
7
32
31
SUS
MGT
HEM

ROW F

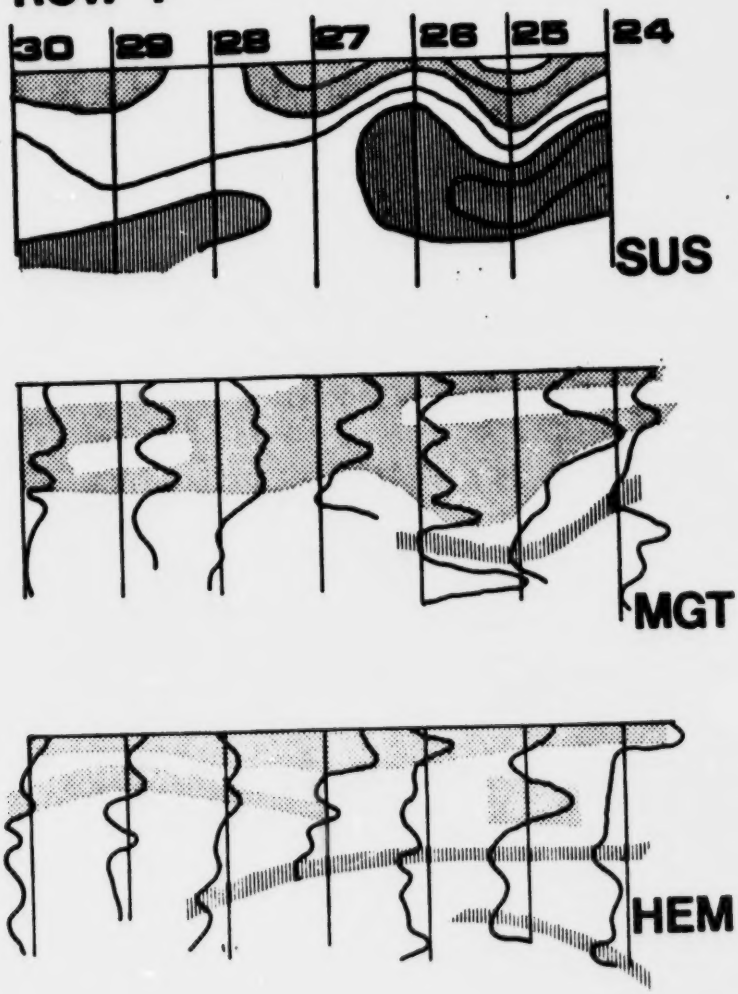

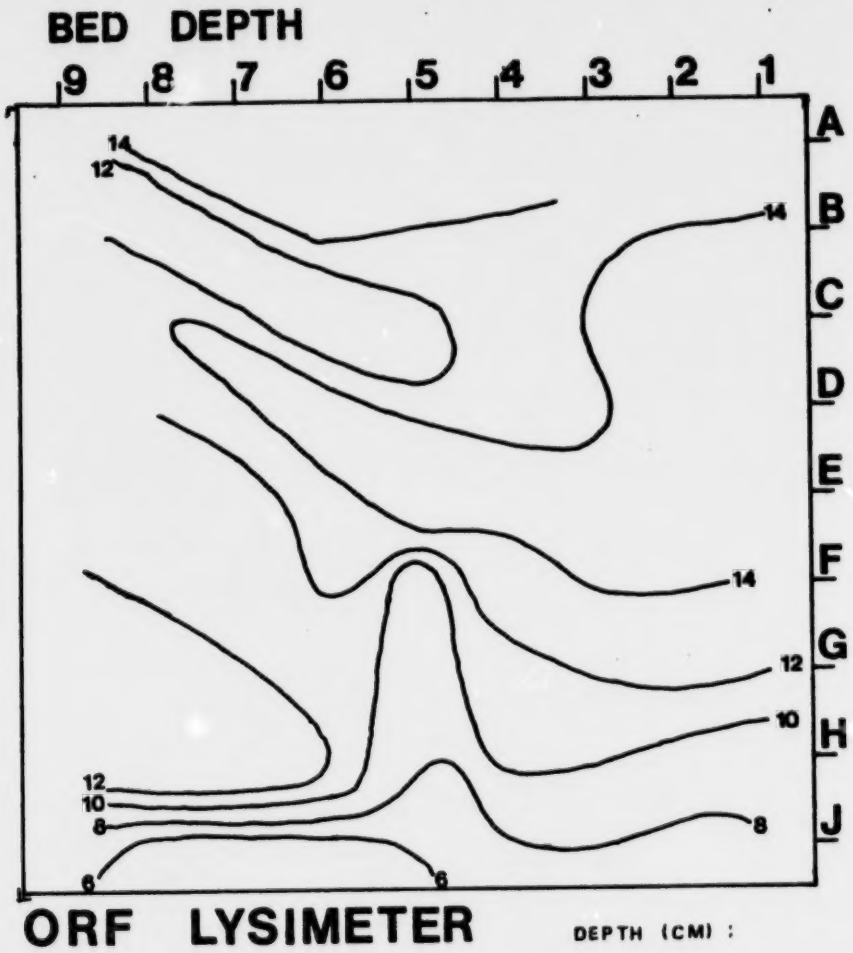


ORF LYSIMETER

DEPTH (CM) :

CONTOUR INTERVAL : 0.5

WATER FLOW : ↓

Table 1 Sulphur uptake measurements

| Site and times of measurements | Period of measurement (h) | Air concentration ($\mu g\ m^{-3}$) | Gaseous fraction (%) | Mean uptake ± s.e.m. ($\mu g\ m^{-2}\ s^{-1}$) | Wind ($m\ s^{-1}$) |
|---|---|---|---|---|---|
| Forest* | | | | | |
| 1030–2000 h | 16 | 6–11 | 60 | <0.01 | 3.2–4.8 |
| 1200–1700 h | 7 | 12–35 | 84 | 0.04 ± 0.02 | 0.8–4.2 |
| Farmland† | | | | | |
| 1200–1730 h | 3 | 3–8 | 50 | 0.03 ± 0.02 | 2.2–5.7 (westerly; peas) |
| 1100–1600 h | 5 | 16–50 | 75 | 0.19 ± 0.02 | 2.2–4.4 (easterly; rye grass) |

* Forest: Crowthorne, Berkshire. 20-yr-old Scots Pine 14 m high unthinned since planting. Flux measurement 3 m above tops. Measurements are for 9 days between 1 and 20 May 1977.

† Farmland: Blewbury, Berkshire. Easterly fetch; Italian rye grass 75 cm; westerly fetch, peas 40 cm. Flux measurement 4 m above soil surface. Measurements are for six days between 21 June and 5 July 1977.

velocity of about 0.2 $cm\ s^{-1}$ for these forest measurements and about 0.6 $cm\ s^{-1}$ for the farmland measurements. All measurements were made in a turbulent atmosphere.

The sulphur detector responds to gaseous and particulate compounds. Particulate sulphur contributes only a fraction of the fluxes reported here, as the sulphate concentration at the field sites, assumed to be similar to that measured at Harwell, was only 20% of the total sulphur at the higher concentrations and the deposition velocity for small particles such as sulphate is much smaller than, or comparable with, that for sulphur dioxide[2,15].

Garland[2] summarises measurements of sulphur dioxide deposition over grass, crops and bare soil made by the profile and radioactive methods that give deposition velocities in the range 0.3–1.2 $cm\ s^{-1}$ with a median value 0.8 $cm\ s^{-1}$, in close agreement with that measured by the eddy correlation method here. Profile measurements in a forest[2] suggested an upper limit of the deposition velocity of 2 $cm\ s^{-1}$. Estimates based on measurements of individual shoots and extrapolation suggest a deposition velocity varying from a daytime maximum value of 0.6 $cm\ s^{-1}$ in the morning to 0.2 $cm\ s^{-1}$ in late afternoon to a night-time value of 0.1 $cm\ s^{-1}$, depending on stomatal resistance (closure) for a dry forest canopy[3]. The measurements presented here for the higher sulphur concentrations suggest a similar low deposition velocity for sulphur on the forest canopy during the afternoon. (We found no evidence of a diurnal variation in surface resistance during the period of our measurements.) Forest measurements were made when the new growth on the forest was just emerging and most of the exposed needles would have been from previous year's growth and are known to display lower uptake rates[3]. Furthermore, the sensible heat flux from the forest was frequently about 50% of the global total incoming solar radiation. This indicates that little evapotranspiration was taking place. The stomatal resistance to gaseous transfer would most probably be high in these conditions. Indeed, stomatal resistance is generally higher during the afternoon[3,16], and the measurements presented here may be for a forest in conditions of maximum resistance to sulphur uptake. The observed fluxes over forest and farmland can be entirely accounted for in terms of sulphur dioxide deposition. However this does not preclude a large deposition velocity for particulate sulphur.

The dry deposition to a dry forest canopy at a mean sulphur dioxide concentration of 10 $\mu g\ m^{-3}$, typical of many rural locations, would be perhaps 2–3 kg sulphur $ha^{-1}\ yr^{-1}$, if the representative deposition velocity is as low as that measured here. This is a significant fraction of the estimated total sulphur deposition in English and Scottish upland sites of 10–20 kg sulphur $ha^{-1}\ yr^{-1}$ (ref. 1). If as suggested[3] gaseous and particulate uptake onto a wet canopy could account for a much larger fraction of the total deposition, then measurements with the method presented here can resolve this question.

We thank L. C. Cox for help with the field work, A. Hadjitofi for developing the sulphur detector, M. M. Davies for programming the computer, C. Healy and Miss J. B. Tarrant for the sulphate analyses, the Director of the Road Research Laboratory and the Manager of Churn Estates farm for access to field sites. I.E.G. thanks the Nuffield Foundation for a Travelling Fellowship and Dr A. C. Chamberlain for his help during the visit. The work was supported by the Department of the Environment.

I. E. GALBALLY

*CSIRO Division of Atmospheric Physics, P.O. Box 77, Mordialloc, Victoria, Australia 3195*

J. A. GARLAND

*Environmental and Medical Sciences Division, AERE, Harwell, Oxfordshire, UK*

M. J. G. WILSON

*Department of Chemical Engineering and Chemical Technology, Imperial College, Prince Consort Road, London SW7, UK*

Received 27 December 1978; accepted 15 May 1979.

1. Department of Environment, Pollution Paper No. 7, *Effects of Airborne Sulphur Compounds on Forests and Freshwater* (HMSO, 1976).
2. Garland, J. A. *Proc. R. Soc.* A354, 245 (1977).
3. Garland, J. A. & Branson, J. R. *Tellus* 29, 445 (1977).
4. Priestley, C. H. B. *Turbulent Transfer in the Lower Atmosphere* (University of Chicago Press, 1959).
5. Desjardin, R. L. & Lemon, E. R. *Boundary-Layer Met.* 8, 475 (1974).
6. Galbally, I. E. *Adv. Geophys.* 18B, 329 (1974).
7. Hicks, B. B. *Boundary-Layer Met.* 3, 214 (1972).
8. Garratt, J. R. *Boundary-Layer Met.* 8, 255 (1975).
9. Hadjitofi, A. & Wilson, M. J. G. *Atmos. Envir.* (in the press).
10. McBean, G. A. *J. appl. Met.* 11, 1078 (1972).
11. Dyer, A. J. & Garratt, J. R. *J. met. Soc., Japan* 56, 19 (1978).
12. Dyer, A. J. & Hicks, B. B. *Q. Jl R. met. Soc.* 98, 206 (1972).
13. Wyngaard, J. C. in *Workshop on Micrometeorology* (ed. Haugen, D. A.) (Am. Met. Soc., 1973).
14. Sreenivasan, K. R., Chambers, A. J. & Antonia, R. A. *Boundary-Layer Met.* 14, 341 (1978).
15. Wesely, M. L., Hicks, B. B., Dannevik, W. P., Frisella, S. & Husar, R. B. *Atmos. Envir.* 11, 561 (1977).
16. Gash, J. H. C. & Stewart, J. B. *Boundary-Layer Met.* 8, 453 (1975).

# Magnetic measurements used to assess sediment influx at Llyn Goddionduon

THE preliminary results of an attempt to estimate sediment influx in a small upland lake using magnetic susceptibility measurements on whole unextruded sediment cores obtained from a grid covering almost the whole area of open water are reported here. The susceptibility variations, reinforced by a wider range of magnetic measurements on individual samples, provide a basis for core correlation over the whole lake. The speed with which such studies can be accomplished makes possible a much more secure empirical basis for calculations of total sediment input versus time than do conventional methods of core correlation and analysis.

0028–0836/79/270050–04$01.00

© Macmillan Journals Ltd 1979

Increasing attention is being devoted to using lake sediments as sources of information about changing ecological processes in the recent past[1,2]. In many cases a large proportion of the lake sediment can be shown to have been derived from the lake watershed. The palaeoenvironmental record may, therefore, often be interpreted largely in terms of changes in the terrestrial ecosystems draining into the lake[3,4]. A prerequisite of fully quantitative studies designed to relate the sedimentary record in the lake to changing material output from its catchment is some procedure for calculating or estimating sediment influx to the whole lake for defined time intervals. Without this procedure all calculations of influx may be biased by the unrepresentative nature of a small number of coring sites.

Empirical attempts to overcome this problem[5] are limited largely by the time-consuming nature of the techniques normally available for core correlation in the absence of synchronous visual stratigraphic markers. Theoretical models developed to allow calculation of total sediment input from a single central core[6], though valuable are unconvincing in view of the numerous unverified assumptions on which they depend.

Thompson *et al.*[7] have shown that magnetic susceptibility measurements of whole, unextruded sediment cores can provide a rapid method of core correlation. The technique leaves the material unaltered, precludes no subsequent study of any kind and can be followed up by a range of related simple, rapid and non-destructive magnetic measurements[8] which often indicate sediment source[9,10] and are directly related to changes in human activity[7,8,11].

Llyn Goddionduon (Fig. 1*a*) lies 244 m above OD in the Gwydyr Forest area of North Wales, ~4 km north-west of Bettws y Coed (G.R. SH 753 586). It covers 6.2 hectares and receives drainage from a catchment of ~25 hectares. Maximum water depth is 6 m, in a small 'trench' occupying <5% of the area of the lake bed. Of the present sediment surface, 50% is between 0.75 m and 4 m deep. A small mire ~0.6 hectares in extent at the southern, outflow, end of the lake represents overgrowth of peat lying partly on marginal lake sediments. Some 25% of the lake is colonised by macrophytes among which *Schoenoplectus lacustris*, *Phragmites communis*, *Eleocharis palustris*, *Nymphaea alba*, *Potamogeton natans* and *Equisetum fluviatile* are the most abundant species[12].

An accurately surveyed grid of 130 minicores[13] was sampled during a 2-week period in July 1977, using a research team varying from five to nine people. Cores were taken at 20 m × 20 m intersections. Where impenetrable substrate precluded this, intermediate cores were taken. In the small trench area an extremely high density of sampling was achieved (27 cores in 950 m$^2$). Whole core susceptibility measurements were carried out on all cores during the same period of field work using a low-field susceptibility bridge[14] temporarily installed in the Drapers Field Study Centre 3.5 km from the lake. Volume susceptibility ($\kappa$) versus depth graph plots were produced

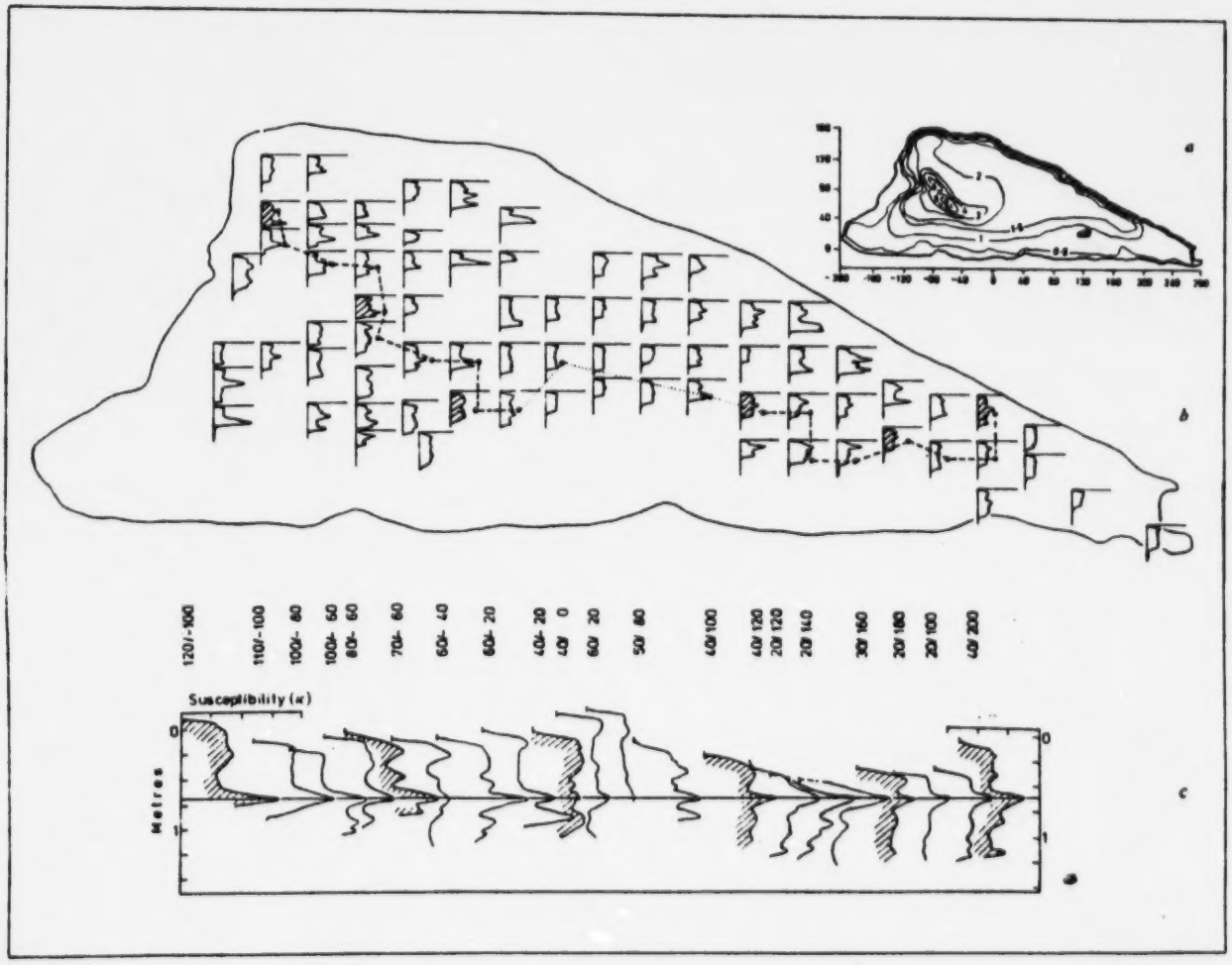


**Fig. 1** Llyn Goddionduon: *a*, Bathymetric map and coring grid coordinates; *b*, whole-core susceptibility traces from the main coring grid. The 'tie-line' joins the cores from which the linked and correlated traces shown below in *c* were obtained. The cores for which single sample $\chi$, SIRM and $\chi$/SIRM ratios are plotted in Fig. 2 are identified by shaded traces.

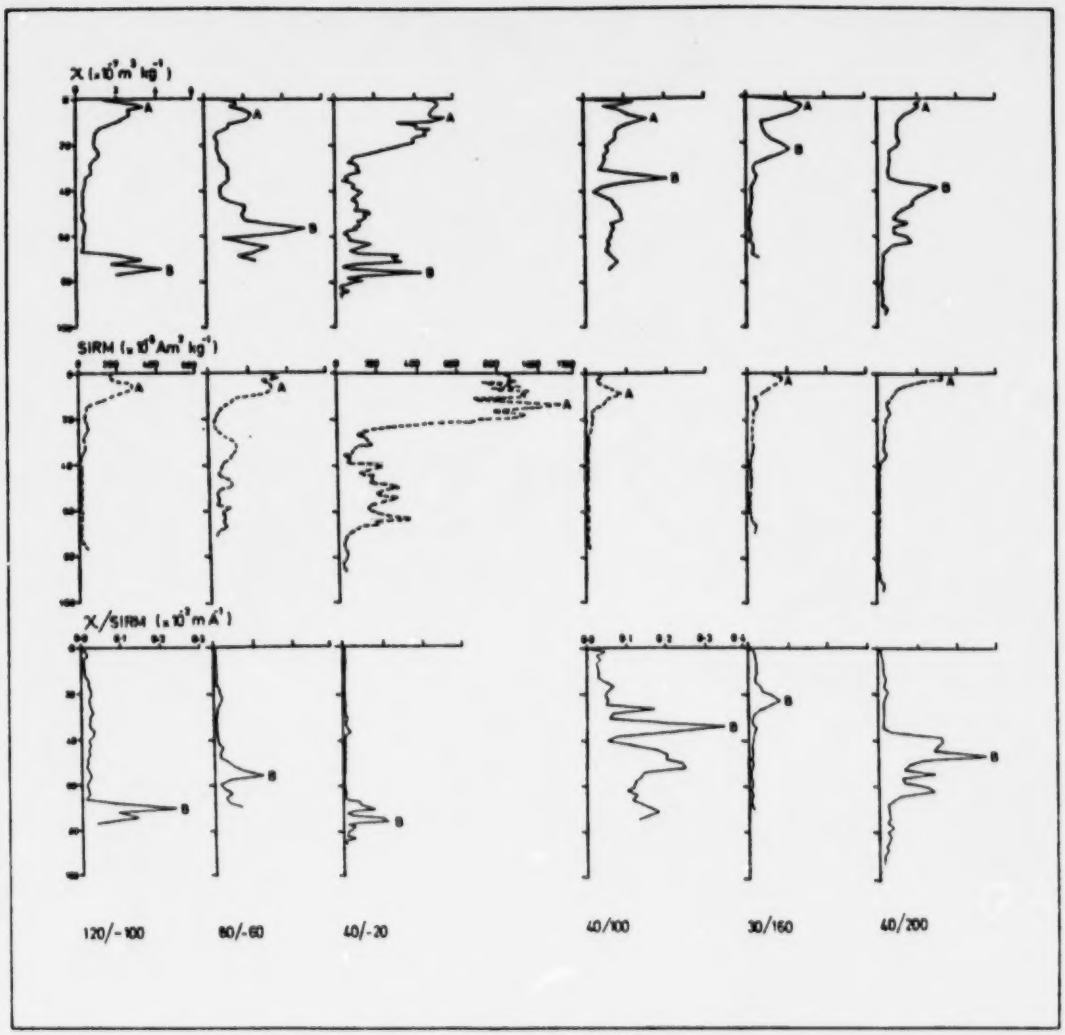


**Fig. 2** Llyn Goddionduon. Single sample plots of $\chi$, SIRM and $\chi$/SIRM for six widely separated cores from the main grid. In all cases, the upper peak in $\chi$ and SIRM which gives low $\chi$/SIRM values corresponds with the influx of magnetic minerals subsequent to a forest fire in 1951. The lower peak is clearly distinguishable from this in all cores by virtue of its high $\chi$/SIRM ratios.

automatically immediately after sensing and it was thus possible to plan day-to-day field sampling priorities in the light of the results obtained within a few hours of taking each set of cores.

Subsequent studies based on extruded sediment have included measurements of specific susceptibility ($\chi$), the intensity and direction of natural remanence (NRM), anhysteretic remanence (ARM), saturation isothermal remanence (SIRM) and coercivity of SIRM ($B_{CR}$). These magnetic measurements provide a wide range of rapidly calculated parameters and ratios which may be used to test core-correlation schemes. In addition chemical, particle size, loss-on ignition, pollen-analytical and radiometric studies are in progress.

Figure 1*b* shows whole core susceptibility traces for a selection of cores from the main grid of cores for the whole lake. In view of the paucity of Flandrian (Post-glacial) sediments in the tiny trench zone (<1 m in all 27 cores from only 5% of the lake), the complex deposition pattern of these cores has little effect on 'whole lake' investigations and the trench results can be satisfactorily assessed on the main 20-m grid. A 'tie-line' has been drawn down the length of the lake. The tie-line cores have been provisionally correlated using the scheme of whole core susceptibility peak matching indicated in Fig. 1*c* and substantiated in more detail by the plots of specific magnetic parameters from dried contiguous 1- or 2-cm subsamples presented in Fig. 2. The central zone in Fig. 1*b* reflects an area of more extended deposition within which the main susceptibility peak used in correlation lies below the depth of sediment penetrated by 1.3-m cores.

Figure 2 shows down core $\chi$, SIRM and $\chi$/SIRM ratios for dried sub-samples in, six widely separated cores located on Fig. 1. Peak $\chi$/SIRM ratios associated with the main tie-line linking the sites, and low $\chi$/SIRM ratios characteristic of the near surface peak (masked by the core tops in whole-core measurements) are common to all the cores and support the proposed correlation scheme. The uppermost sediment with low $\chi$/SIRM ratio is attributable to the forest fire of 1951 (ref. 11) which occurred on the north-east edge of the drainage basin.

Studies in progress are designed to confirm the full pattern of correlation, to date each stage in accumulation, to characterise sedimentologically, chemically and magnetically the variations in deposition rate portrayed, and to relate them to the history of land use at the site decipherable in the pollen record. These studies will provide a basis for empirically based calculations of changing net sediment input versus age for almost all the lake basin for the time interval spanned by the majority of the cores.

Magnetic measurements now open up the prospect of core scanning and correlation with a speed, and on a scale, orders of

magnitude greater than conventional techniques allow. Well founded empirical calculations of total sediment input versus time thus becomes feasible even for lakes as complex as the present example. In the case of Llyn Goddionduon the anticipated pattern of sediment focusing into what is at present the deepest part of the lake has not been characteristic of the Flandrian period. Nevertheless, correlatable patterns emerge from the magnetic studies even within and between zones of relatively shallow marginal deposition.

We thank the NERC, the Leverhulme Trust and the Universities of Liverpool and Edinburgh for financial support, also colleagues and students from both Universities for field assistance, and we are grateful for the facilities in the Draper's Field Centre, Rhyd-y-Creuau.

J. BLOEMENDAL
F. OLDFIELD

*Department of Geography, University of Liverpool, Liverpool, UK*

R. THOMPSON

*Department of Geophysics, University of Edinburgh, Edinburgh, UK*

Received 6 March; accepted 24 May 1979.

1. Battarbee, R. W. *Phil. Trans. R. Soc.* B **281**, 303 (1977).
2. Pennington, W., Cambray, R. S., Eakins, J. D. & Harkness, D. D. *Freshwat. Biol.* **6**, 317 (1976).
3. Mackereth, F. J. H. *Phil. Trans. R. B* **250**, 165 (1966).
4. Oldfield, F. *Prog. Phys. Geogr.* **1**, 460 (1977).
5. Davis, M. B. *Envir. Conserv.* **3**, 130 (1976).
6. Lehman, J. T. *Quat. Res.* **5**, 541 (1975).
7. Thompson, R., Battarbee, R. W., O'Sullivan, P. E. & Oldfield, F. *Limnol. Oceanogr.* **20**, 687 (1975).
8. Oldfield, F., Dearing, J., Thompson, R. & Garrett-Jones, S. E. *Pol. Arch. Hydrobiol.* **25**, 321 (1978).
9. Oldfield, F., Rummery, T. A., Thompson, R. & Walling, D. E. *Water Resources Res.* (in the press).
10. Longworth, G. *et al. J. Soil Sci.* (in the press).
11. Rummery, T. A., Bloemendal J., Dearing, J., Oldfield, F. & Thompson, R. *Ann. Geophys.* (in the press).
12. Liddle, M. J. *A Survey of Twelve Lakes in the Gwydyr Forest Region of Snowdonia.* (University College of North Wales, 1974).
13. Mackereth, F. J. H. *Limnol. Oceanogr.* **14**, 145 (1969).
14. Molyneux, L. & Thompson, R. *Geophys. J. R. astr. Soc.* **32**, 429 (1973).

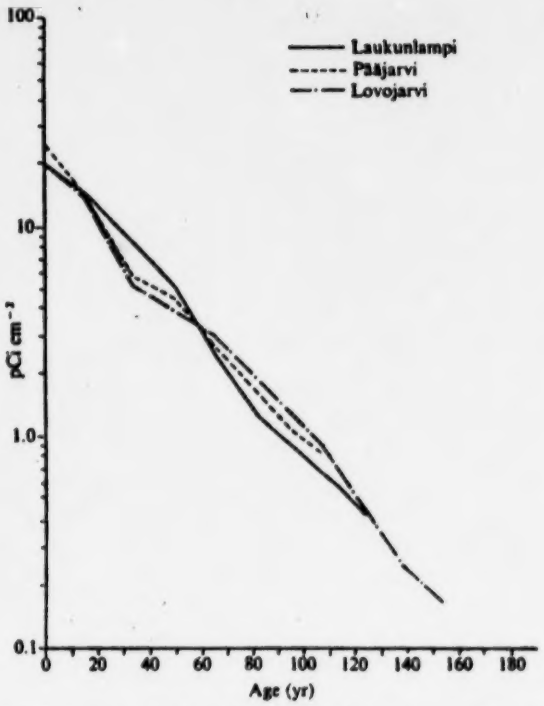


**Fig. 1** Cumulative residual unsupported $^{210}$Pb versus age in three annually laminated sediment profiles from lakes in east Finland. The approximation to a negative exponential function in each case confirms the validity of this as the appropriate dating parameter.

# $^{210}$Pb dating of annually laminated lake sediments from Finland

USE of $^{210}$Pb dating is increasing rapidly and applications include studies of accelerated eutrophication in major lakes[1], salt-marsh accretion[2], the recent history of heavy metal pollution[3] and accelerating soil erosion resulting from subsistence agriculture[4]. As dating models have increased in variety and complexity, it is important to compare models against precise and unambiguous independently derived time scales. In each area of application of $^{210}$Pb dating, the inferences drawn from the calculated age–depth curves and the estimates of changing flux rates are often highly dependent on the $^{210}$Pb dating model used. In this report $^{210}$Pb-derived estimates of lake sediment age and dry-mass sedimentation rates are compared with ages and rates calculated directly by counting annual laminations. The results support a model of $^{210}$Pb dating which assumes a constant net rate of supply (c.p.s.) of unsupported $^{210}$Pb to the sediment despite fluctuations in dry mass sedimentation rates. Our findings underline the need for empirical evaluation of alternative $^{210}$Pb dating models in the widest possible range of contexts. They also cast doubt on some published studies in which strongly 'kinked' profiles of unsupported $^{210}$Pb concentration have been interpreted within the framework of conventional constant initial concentration (c.i.c.) assumptions.

Most workers using $^{210}$Pb dating have assumed the initial unsupported $^{210}$Pb concentration to be constant throughout a dated profile, or at least in large sections of the profile. This assumption can be satisfied in theory by a direct association between sedimentation and unsupported $^{210}$Pb supply[5], or by a combination of constant unsupported $^{210}$Pb flux and constant dry-mass sedimentation for all of[6], or segments[7] of, each profile. Authors using c.i.c. models have dealt with sharply inflected or non-monotonic $^{210}$Pb-versus-depth profiles, or individual 'anomalous' values, by invoking alternative explanations such as physical mixing[8], bioturbation[9], diffusion[10] and co-precipitation of $^{210}$Pb with manganese[11]. Where authors have referred to the alternative basic assumption of a constant net rate of supply (c.r.s.) of unsupported $^{210}$Pb to the sediment independent of fluctuations in bulk sedimentation rate this alternative has usually been dismissed in favour of some variant of the c.i.c. model[12,13], or else it has been used but not empirically tested in a rigorous manner[2,14,15]. Recent applications of c.r.s. model calculations[16] to lake sediment sequences in Northern Ireland, the Highlands of Papua New Guinea[17] and Lake Michigan[18] provide strong, varied, but essentially circumstantial evidence for the validity of c.r.s.-derived age–depth relationships and dry-mass sedimentation rates. In each of these case studies, as in the example by Robbins[15], the choice between alternative models has a major impact on the results and their interpretation.

The sites from which the present evidence has been obtained provide a very precise and unambiguous basis for testing the alternative dating models. Not only are their recent sediments in the form of distinctive annual laminations, confirmed both biostratigraphically[19,20] and by $^{239,240}$Pu and $^{137}$Cs analyses (T. Jaakola, K. T., P. H. and S. Tiainen, unpublished), but they have also experienced disturbance in each catchment which has given rise to fluctuations in sedimentation rate strong enough to 'kink' the unsupported $^{210}$Pb concentration-versus-depth curve.

In the c.r.s. model, the age $t$ of sediments of depth $x$ is calculated from[16]

$$A(x) = A(0)\,e^{-\lambda t} \qquad (1)$$

0028-0836/79/270053—03$01.00

© Macmillan Journals Ltd 1979

IAEA SM-208/38

# APPLICATION OF MAGNETIC SUSCEPTIBILITY MEASUREMENTS TO URANIUM EXPLORATION IN SANDSTONES

P.L. HAFEN, S.S. ADAMS, G.B. SECOR
The Anaconda Company,
Salt Lake City, Utah,
United States of America

Abstract

APPLICATION OF MAGNETIC SUSCEPTIBILITY MEASUREMENTS TO URANIUM EXPLORATION IN SANDSTONES.

The paucity of magnetite and ilmenite in proximity to certain uranium deposits in permeable sandstones has been noted. Studies indicate that these detrital magnetic minerals were destroyed by the same processes which formed the uranium deposits. The antipathy between uranium deposits and magnetite and ilmenite suggests that magnetic susceptibility measurements may be useful in uranium exploration. To evaluate this possibility, a series of magnetic susceptibility measurements were made both on outcrops and samples collected from drill holes, close to and remote from known uranium deposits. These data indicated that variations in the magnetite-ilmenite content of typical sandstones can be reliably measured. Down-hole magnetic susceptibility measurements have also been successfully correlated with magnetite-ilmenite concentrations in drill core and cuttings. A down-hole probe has been used in sandstone exploration programmes and has provided a reliable, convenient method for collecting information on the distribution of detrital ilmenite and magnetite. This information, when compared with the cuttings, stratigraphic information, gamma-ray and resistivity logs, provides an additional guide in determining the favourability of certain sandstones for the occurrence of significant uranium deposits.

## INTRODUCTION

Fluvial and marginal marine sandstones host a substantial percentage of the world's uranium reserves. Within these sandstones, uranium deposits are commonly associated with detrital or redistributed carbonaceous material and/or authigenic sulfides formed in the organic-bearing sediments. Minor amounts of detrital magnetite and ilmenite are also common constituents of these sands. Studies of one such fluvial sandstone sequence, the Jurassic Morrison Formation of northwestern New Mexico, revealed that detrital magnetite-ilmenite grains have been altered and largely destroyed in the host sands in the vicinity of primary uranium deposits. It was suggested that this alteration, described and interpreted by Adams et al. [1], might prove a useful exploration guide. Since magnetite and ilmenite are magnetic, susceptibility measurements should indicate the favorability of a sandstone for the occurrence of uranium deposits.

This paper presents data and observations related to the use of magnetic susceptibility measurements in uranium exploration in northwestern New Mexico. Magnetic susceptibility measurements were made on outcrops of potential uranium host rocks, samples of cuttings and core from exploration drill holes, and, ultimately, in exploration holes with a down-hole magnetic susceptibility tool developed by the U. S. Bureau of Mines. These measurements were designed to determine 1) if variations

in the concentration of magnetite-ilmenite, in the range of trace to one-half percent, could be detected in the sandstones, 2) if concentration variations in magnetic heavy minerals resulting from depositional processes and post-depositional alteration could be resolved, and 3) the magnitudes of magnetic susceptibilities of rocks associated with sandstone uranium deposits.

The use of the magnetic susceptibility probe of the U. S. Bureau of Mines for logging several uranium exploration holes is gratefully acknowledged as are useful discussions with their staff regarding the performance and specifications of the probe. This paper is presented with the permission of The Anaconda Company.

## MEASUREMENTS OF MAGNETIC SUSCEPTIBILITY

### Rock Outcrop Measurements

A series of magnetic susceptibility measurements were made on outcrops of Cretaceous, Jurassic, and Triassic sedimentary rocks in the San Juan Basin of northwestern New Mexico (Figure 1). The measurements, summarized in Figure 2, were performed on outcrops with a field portable Bison Magnetic Susceptibility Bridge.

Dakota Formation - The basal Cretaceous Dakota Formation is a quartzose, fine- to medium-grained, well-sorted sandstone which contains abundant particulate organic material. The low magnetic susceptibilities (0 to 24 μcgs), with an average of 6 μcgs[1], suggest low concentrations of magnetic minerals.

Morrison Formation, Jackpile Sandstone Member - The Jackpile sandstone member of economic usage, which immediately underlies the Dakota Formation, is predominantly sandstone with minor interbedded siltstone and mudstone. In the Jackpile Mine area (see Figure 1), the member ranges in thickness from 30 to 70 meters. The sandstones have been pervasively reduced by detrital and redistributed carbonaceous material and possibly by reductants derived from the overlying organic-rich Dakota Formation. The magnetic susceptibilities range from 2 to 32 μcgs. The average susceptibility for the Jackpile in the mine area is 18 μcgs.

Along the southeastern flank of the San Juan Basin, the Jackpile sandstone is generally less than 30 meters thick and better sorted than in the Jackpile Mine area. Magnetic susceptibilities range from 0 to 27 μcgs. The average of 30 readings is 10 μcgs. Destruction of detrital magnetite-ilmenite is more complete than at the Jackpile Mine area, possibly due to a lack of lithologic heterogeneity resulting in greater internal permeability and possibly greater hydrologic continuity with the overlying organic-rich Cretaceous sediments.

Morrison Formation, Westwater Canyon Member - Where sampled along the western, southern, and southeastern flanks of the San Juan Basin, the Westwater Canyon ranges in thickness from 30 to 100 meters and is composed of sandstone with subordinate interbedded mudstone. It is separated from basal Cretaceous rocks by the relatively impermeable siltstones and mudstones of the Brushy Basin Member which is 16 to 70 meters thick.

[1] Magnetic susceptibility in cgs units × $4\pi$ = magnetic susceptibility in SI units.

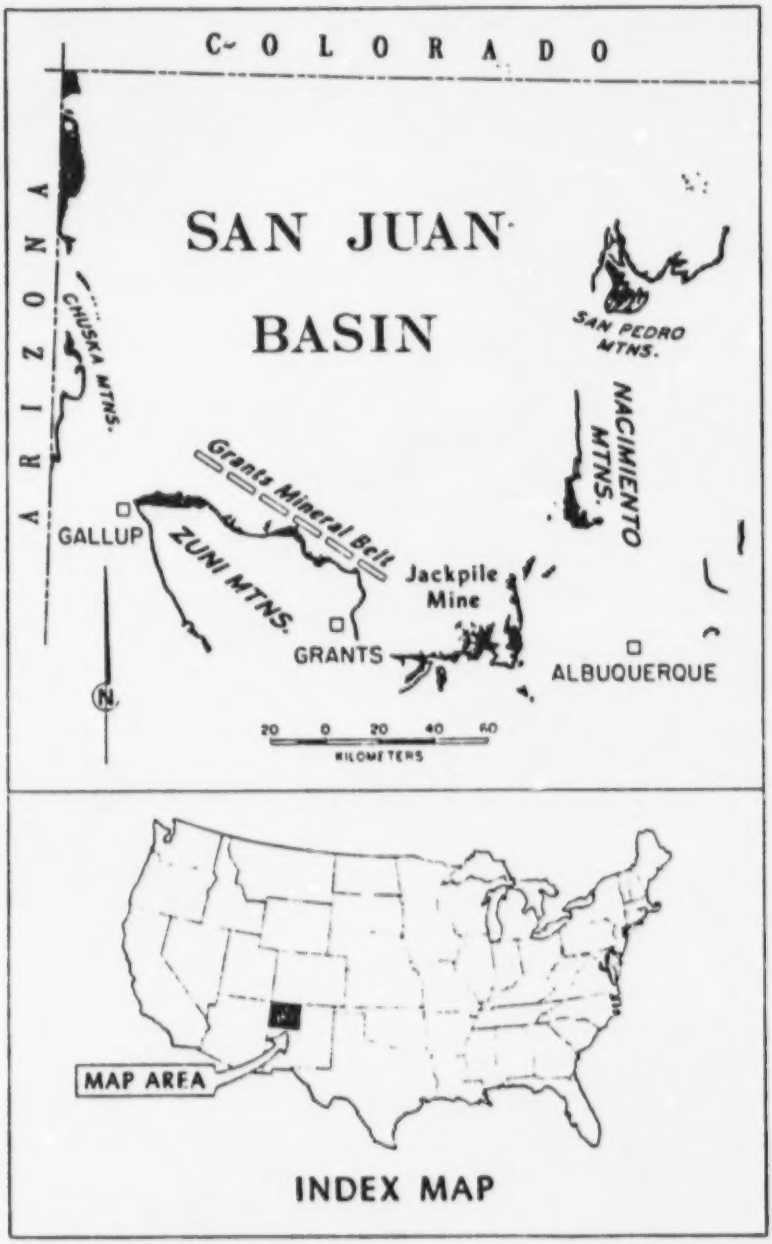


*FIG.1. Location map for outcrops of the Morrison Formation, San Juan Basin, Northwest New Mexico.*

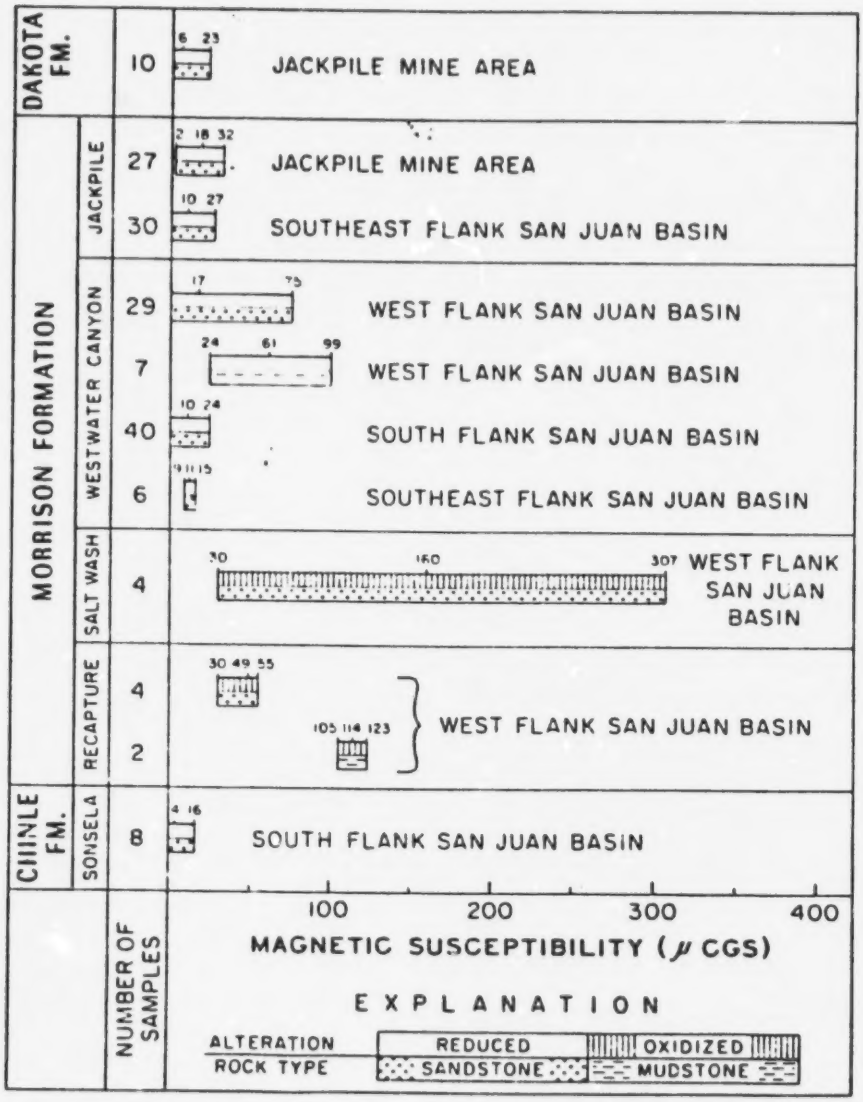


*FIG. 2. Magnetic susceptibility measurements for formation outcrops, San Juan Basin, Northwest New Mexico. The maximum, minimum, and average μcgs are given for each sample group.*

Magnetic susceptibilities for the Westwater Canyon Member show greater variability than for either the Dakota or Jackpile sandstones, presumably reflecting irregular post-depositional alteration due to variations in permeability and the intensity of post-depositional reducing environments. The intensity of magnetite-ilmenite alteration has, therefore, not been uniform. Generally higher magnetic susceptibility values were obtained from mudstone units (average 61 μcgs), whereas the average values for sandstone units from different areas ranged from 10 to 17 μcgs, with considerable variability for individual samples. The higher values for the mudstones and siltstones presumably reflect the original detrital magnetite-ilmenite content which, due to the low permeability of these finer-grained rocks, has been protected from alteration and destruction. The low but variable magnetic susceptibility for the sandstones reflects the widespread, albeit incomplete, post-depositional destruction of magnetite-ilmenite in these sands.

Morrison Formation, Salt Wash Member - Magnetic susceptibility measurements made on red sandstones of the Salt Wash along the west flank of the San Juan Basin ranged from 30 to 307 μcgs. The Salt Wash in this area is interpreted to have never been subjected to significant reducing conditions and, accordingly, no significant alteration of detrital magnetite-ilmenite has occurred. The average magnetic susceptibility of Salt Wash sandstones tested was 160 μcgs.

Morrison Formation, Recapture Member - The magnetic susceptibility of Recapture sediments ranged from a low of 30 μcgs in light-gray sandstones to 123 μcgs in red-brown mudstones. The light-gray sandstones have been subjected to local reducing conditions and partial destruction of detrital magnetite-ilmenite, whereas the red-brown mudstones have never been exposed to significant reducing conditions. The average magnetic susceptibility of the sandstones is 49 μcgs. The average susceptibility for the mudstones is 114 μcgs, suggesting generally negligible post-depositional alteration of detrital magnetite-ilmenite grains.

Chinle Formation, Sonsela Sandstone Bed - Sonsela sandstone beds, exposed along the south flank of the San Juan Basin, are very light gray to light pinkish gray. Interbedded with the sandstones are thin green and gray-green mudstones. Magnetic susceptibility measurements of the sandstone beds range from 1 to 16 μcgs with an average of 4 μcgs, indicating negligible magnetic mineral content and, as substantiated by the color of the sediments, a history of strong reduction and iron dissolution.

Magnetic susceptibility measurements made on outcrops of Cretaceous, Jurassic, and Triassic sediments exposed around the southwest, south, and southeast flanks of the San Juan Basin appear generally consistent with the oxidation-reduction history of these rocks as inferred from the color of the sediments. Magnetic susceptibilities taken within individual sandstones at specific locations yield similar results, whereas measurements in adjacent but distinctly different beds, may, especially where field evidence suggested distinctly different oxidation-reduction histories, yield vastly different susceptibilities. Variations in the permeability of sedimentary units, as inferred from sorting and distribution of fine detrital components, correlate well with variations in magnetic susceptibility.

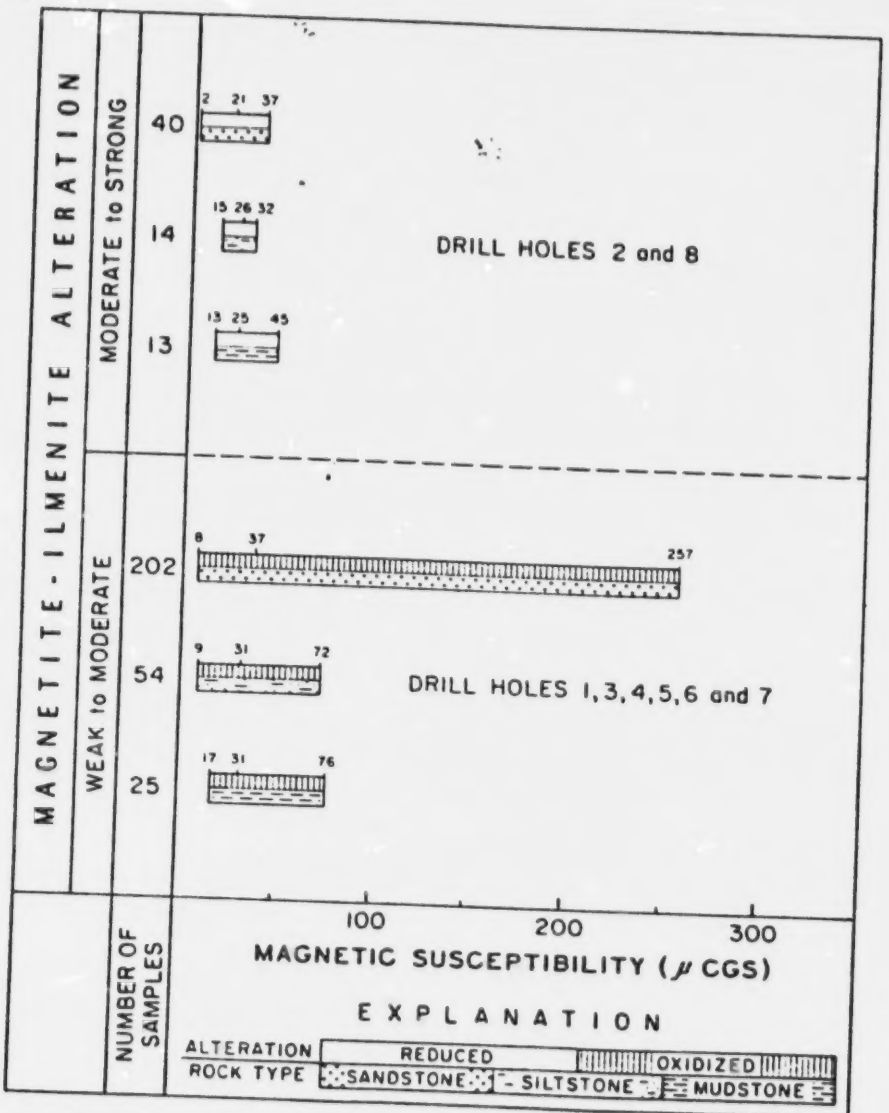


*FIG. 3 Magnetic susceptibility measurements and magnetite ilmenite alteration for core samples from holes drilled in the San Juan Basin, Northwest New Mexico. The maximum, minimum, and average μcgs are given for each sample group.*

## Drill Core Measurements

The magnetic susceptibility of drill core samples of the Westwater Canyon sandstone from eight wide-spaced drill holes in the San Juan Basin was measured with the Bison Magnetic Susceptibility Bridge. The core was sampled and measured at two-foot intervals. These samples were also studied under the binocular microscope and, in some cases, in thin section to determine the degree of magnetite-ilmenite alteration. The results of these measurements, together with data on the alteration, are presented in Figure 3. Thin section studies, noting in particular the alteration of detrital magnetite-ilmenite grains and the types and distribution of authigenic iron and titanium phases, are believed to be the most reliable method of interpreting the oxidation-reduction history of a sediment. Such studies have led to the alteration observations presented in Figure 3 and discussed below.

The magnetic susceptibility of sandstones has a greater range than does the susceptibility of the less permeable siltstones and mudstones, reflecting both the irregular sedimentary distribution and the post-depositional alteration of the detrital magnetite minerals. In particular, the wide ranges in the values for sandstones probably indicate both locally high concentrations, such as heavy mineral horizons and zones of intense iron leaching and destruction of magnetite-ilmenite. The data for drill holes 2 and 8 (Figure 3) indicate that, where the permeable sandstones are interpreted to have been pervasively reduced, magnetic susceptibility variations are small (25 and 22 μcgs respectively) compared to the wider variations in the other six drill holes (71 to 247 μcgs). Also, the average magnetic susceptibility for sandstone in drill holes 2 and 8 are 19 and 24 μcgs, compared to averages from 34 to 42 μcgs for the less altered sandstones in the other six holes.

These data suggest that 1) the relative concentration of ferromagnetic minerals (less than 0.5 wt. %) can be measured, even at their low abundances in the Westwater Canyon Member, 2) depositional variations in the magnetite-ilmenite concentrations in the sandstones can be measured, 3) sandstone intervals in which post-depositional destruction of magnetite-ilmenite has occurred can generally be identified, 4) variations in magnetic susceptibility can generally be related to megascopic or microscopic evidence of sandstone alteration, and 5) alteration of detrital magnetic minerals is more intense, albeit erratic, in sandstones than in the less permeable siltstones and mudstones.

Magnetic susceptibility measurements of outcrops and drill core correlated sufficiently well with the distribution of magnetite-ilmenite, as determined from examination of thin sections and cuttings, to warrant testing a down-hole magnetic susceptibility probe. Accordingly, a down-hole test program was initiated.

## Down-Hole Measurements

Three devices for measuring down-hole magnetic susceptibility were investigated during the early stages of these studies. These tools were developed by the United States Geological Survey, Bureau of Mines, and Atomic Energy Commission. Of the three, the down-hole probe utilized by the Bureau of Mines and designed, in part, by that group appeared the most applicable. This tool was, among its other attributes, the most

sensitive of the three probes, being able to measure changes in susceptibility of 1 μcgs. Arrangements were made with the Bureau of Mines to test the tool in four uranium exploration holes in the San Juan Basin.

Down-hole magnetic susceptibility measurements obtained with the Bureau of Mines' probe correlated exceptionally well with the concentrations of the detrital magnetite-ilmenite observed in cuttings. This correlation, in fact, suggested there had not been significant contamination of cuttings during drilling. In one of the drill holes, a duplicate log was run with good repeatability. The logs also verified that low concentrations of magnetite-ilmenite could be measured reliably with the probe. The probe experienced, however, significant thermal drift during the logging of the holes. These results were sufficiently encouraging to proceed with the development of a probe of our own specifications.

The Anaconda probe was designed or subsequently modified to the specifications in Table I. The susceptibility device employs a Maxwell bridge circuit with a laminated ferrite core. The flux gathering ability of the ferrite is temperature sensitive, requiring internal thermal stabilization to minimize the effects of variable bore hole temperatures. The method used to achieve thermal stability involves 2 cm of insulation around the core and nichrome wire heaters to raise the temperature of the core above bore hole temperatures. In practice, periodic up-hole monitoring of the core temperature improves the efficiency of the logging operation.

Calculations indicate that approximately 95 percent of the in-balance signal originates from within 19 cm of the axis of the core. This implies that the position of the probe with respect to the walls of the drill hole, as well as variations in hole diameter, will have an effect on the signal strength. Part of this potential problem has been eliminated by stabilizing the probe in the center of the hole. Caliper logs are not generally run so that variations of the bore hole diameter are not taken into consideration.

At the present time, recording is done only in an analogue mode on a two trace recorder. Calibration spikes equivalent in amplitude to the mid-range of the particular scale are superimposed on the traces of the record automatically or manually at the discretion of the operator. During the past three years, this probe has been used in a number of different geological environments. Problems experienced during testing have required modifications to minimize thermal drift, improve sensitivity, and to position the probe in the hole. The modifications have largely eliminated the difficulties through the addition of a fiberglass shroud for thermal insulation of the coil portion of the probe; the sensitivity has been increased through a number of alterations; and a simple device has been developed to keep the probe centered in drill holes during logging operations.

In recent operation, log repeatability for zones containing magnetite is good although the magnitude of the magnetic susceptibility is somewhat variable. The probe has not been calibrated absolutely because relative concentrations of the detrital magnetic minerals are adequate for the interpretation of diagnostic alteration.

Figure 4 is a reproduction of a magnetic susceptibility log for an exploration drill hole. Also shown is the lithology for the Morrison

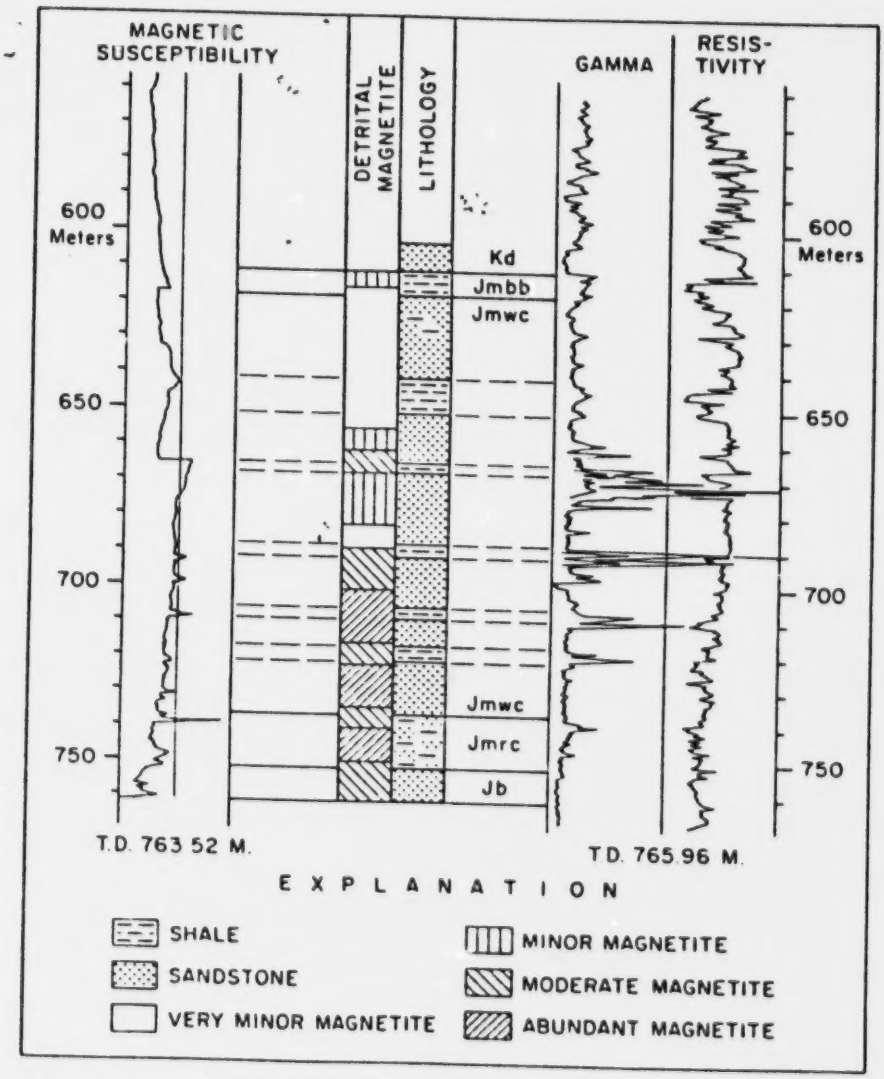


*FIG 4. Correlation of a typical down-hole magnetic susceptibility log with gamma-ray and resistivity logs, lithology, and the distribution of magnetite in the Morrison Formation.*

*Cretaceous:*

*Kd = Dakota formation.*

*Jurassic:*

*Jmbb = Morrison Formation, Brushy Basin Member*

*Jmwc = Morrison Formation, Westminster Canyon Member.*

*Jmrc = Morrison Formation, Recapture Creek Member*

*Jb = Bluff Formation.*

*T.D. = total depth.*

interval, together with a resistance log and the detrital magnetite content as determined from cuttings. Background drift is apparent in the magnetic susceptibility log. This drift results from temperature differences in the formation waters. Higher concentrations of magnetic minerals are indicated by peaks on the magnetic susceptibility log. Of particular note is the erratic but higher concentration of magnetic minerals in the lower one-third of the Morrison Formation. This is substantiated by the distribution of magnetite-ilmenite observed in the cuttings. Also of interest is the excellent correlation between higher magnetite-ilmenite concentrations and shale horizons within the Morrison Formation.

## CONCLUSIONS

Magnetic susceptibility measurements on formation outcrops and drill core have demonstrated that relative concentrations of detrital magnetic minerals can be reliably measured in the sandstones of the San Juan Basin. In most cases, the measured magnetic susceptibility could be related to the alteration of the sandstone, in particular the destruction of magnetite-ilmenite as interpreted from the lithologic characteristics of the sediments and verified by thin section examination. Down-hole magnetic susceptibility measurements correlated well with the distribution of magnetite-ilmenite in drill hole cuttings. These observations supported the development of a modified down-hole tool which can measure the relative distribution of magnetite-ilmenite in uranium exploration drill holes more rapidly and reliably than similar information can generally be obtained from drill hole cuttings. As the destruction of detrital magnetite-ilmenite is believed related to processes responsible for the formation of the uranium deposits, this data is useful in prospecting for a major type of uranium deposit, particularly where drill hole cuttings are unavailable or contaminated.

## REFERENCE

[1] ADAMS, S. S., CURTIS, H. S., HAFEN, P. L., "Alteration of detrital magnetite-ilmenite in continental sandstones of the Morrison Formation, New Mexico," in Formation of Uranium Ore Deposits (IAEA Symposium, Athens, Greece, 1974) 219-253.

## DISCUSSION

J.H. SCOTT. What do you mean by "operator assist" in Table I?

S.S. ADAMS. By operator assist I mean that manual adjustments are made.

J.H. SCOTT: According to the specifications for your magnetic susceptibility probe, thermal drift is less than 5% of full scale per hour with operator assist. Does this mean that the drift is only 20 μcgs units per hour on the most sensitive scale (−100 to +300 μcgs)?

S.S. ADAMS. The design specifications were for a limit of 5% drift. The initial performance fell short of specifications and although improvements have been made drift is still not controlled as well as expected.

H. MÜLLER: Have you any experience with measurements in deposits without radioactive equilibrium, or without any daughter products?

S.S. ADAMS: No. Parts of some of the deposits in the Morrison Formation are out of equilibrium due to leaching and redistribution of uranium. The patterns of magnetite-ilmenite destruction, hence the magnetic susceptibility, correspond to the original uranium distribution in the sandstone.

TITLE

# MEASUREMENT OF MAGNETIC SUSCEPTIBILITY ON TAILINGS CORES

## REPORT ON CORES FROM CANMET LYSIMETERS A AND C

Work on this project was conducted under the auspices of the National Uranium Tailings Program of the Canada Centre for Mineral and Energy Technology, Energy, Mines and Resources, Canada.

DSS File No. 15SQ.23241-4-1648

DSS Contract Serial No. OSQ84 - 00103

CANMET PROJECT NO.

CANMET SCIENTIFIC AUTHORITY: Mr. G. M. Ritcey

OCTOBER 1984

## INTRODUCTION

Six cores from two lysimeters, three each, located at the CANMET facilities in Ottawa have been examined for magnetic susceptibility variations with depth. Like the previous study of cores from the ORF lysimeter all measurements were made on the full core enclosed in its ABS plastic container. Again a Sapphire Instruments SI-1 susceptibility bridge was used for all measurements. This study though used a different pass-through coil with dimensions of 2.5cm width, and 7.5cm diameter opening. The result of this coil change was implemented first to permit measurement of the CANMET cores without removing them from the plastic piping. And second, the narrower coil means that each measurement is less dependent on its immediate adjacent measurement. Using the 7.5cm wide coil, meant that points in the centre of the core are integrated into the susceptibility reading three times when using a sequential 2.5cm spacing of measurement points. In effect the broader coil may be averaging out some of the detail present in the core.

No attempt has been made to cross-calibrate the new narrow coil to the old 7.5cm wide coil. The susceptibility readings as treated in this study are examined relative to a lysimeter average value. For lysimeter A the log mean susceptibility value is $13.7 \times 10^{-6}$ emu, while for lysimeter C the log mean susceptibility value is $16.4 \times 10^{-6}$ emu. Individual susceptibility

values examined relative to the lysimeter average permit the recognition of zones of relative oxide depletion, or enhancement.

As with the previous study each observation point was measured five times, and each time the coil was zeroed immediately before taking each reading. From these five readings a log mean value was calculated which is considered truly representative of the susceptibility at the point of observation. In all cases the standard deviation of the five readings is two orders of magnitude less than the average value. The values quoted in Tables 1 and 2 are defined as $\log_{10}$ (Observation point mean value $\times 10^{+6}$) - $\log_{10}$ (log mean average susceptibility $*10^{+6}$ for the whole lysimeter).

Because of the larger sample size of the previous collection it was possible to examine that data base in terms of a normal population frequency distribution. This procedure revealed the presence of four separate populations relating to different states of oxidation/reduction of the tailings. Unfortunately there are too few observation points in this collection to construct a meaningful cumulative frequency plot for either, or both of the two Ottawa lysimeters.

All data plots use the top surface of the tailings, in the absence of any other absolute frame, as the reference horizontal surface. Should there be some topography on the top of the bed then this is carried through all the correlated levels.

## RESULTS

Tables 1 and 2 present the details of the susceptibility difference values found in lysimeters A and C located in Ottawa.

Again we have made the assumption that at the time of initiation the tailings in the lysimeter were completely homogeneous. So that any susceptibility differences now observed are the result of processes active during the operation of the lysimeter. The overall log mean susceptibility values for the two lysimeters are statistically different; A being 13.7 $x10^{-6}$ emu and C being 16.4 $x10^{-6}$ emu. Reasons for this discrepancy may include; a) different sources of the tailings in the two lysimeters; b) if of the same tailings source then it is possible that some oxide separation took place upon initiation of the lysimeters; and c) this discrepancy may reflect the total removal of some iron species in one lysimeter relative to the other.

Figure 1 and Table 1 present the data obtained for lysimeter A. There are three distinct features present in this plot.

1) The top surface zone is strongly depleted relative to the lysimeter average. This zone appears to be approximately 5cm thick. Strongest depletion is found at the corners of the lysimeter. This may be signifying that there is drainage in towards the centre of the lysimeter. The centre being less depleted because some of the oxides migrating towards this zone were entrained by silicate particles.

2) Zone 2 extends from approximately 5cm (level 3) to approximately 25cm (level 10). The upper 5cm of this zone is really a transition between zones 1 and 2, that is from depleted susceptibility levels, the values rapidly change to enhanced susceptibility levels. Over the next 20cm of zone 2 all three zones show a simple progressive logarithmic reduction in susceptibility level. It is probable that this distribution reflects the deposition of oxides scoured from Zone 1 and deposited in Zone 2. Once deposition commences it is anticipated the majority of oxides in suspension will be deposited rapidly. As the transport distance increases gradually less and less oxides are retained in suspension - hence the decreasing enhancement of susceptibility signal. Throughout the central core has systematically lower values than the two peripheral cores. Flow rates in the centre of the lysimeter are probably higher than at the margins of the lysimeter.

3) Zone 3 extends form 25cm (level 10) to the base of the lysimeter at 32.5cm (level 13). At the corners of the lysimeter Zone 3 is represented by an increase to enhanced susceptibility levels. At the centre of the lysimeter the susceptibility level becomes depleted. This distribution can be explained by having the drain located at the centre of the lysimeter, which would make the corners into regions of low flow rate, and hence the location of relative oxide deposition.

Figure 2 and Table 2 presents the results obtained for lysimeter C. This data shows some similarities and some disimilarties to the results obtained from lysimeter A.

Like lysimeter A, lysimeter C also contains a surface zone of significant oxide depletion. At the centre of the lysimeter this depleted zone extends down to 10cm (level 4). At the S. W. corner is only extends 5cm (level 2) and the N. E. corner only 2.5cm (level 1).

Below this surface susceptibility reduced zone lysimeter C does not show the same systematic changes as shown by lysimeter A. It appears more as if each core has its own distinct pattern of susceptibility distribution. The core from the N. E. corner of lysimeter C is the one that most closely approximates to the pattern found in lysimeter A. At a depth of 5cm (level 2) the N.E. core has strong positive susceptibility level which gradually diminishes increasing depth. Negative values are found between 20cm (level 8) and 27.5cm (level 11). A small positive zone is found at the bottom level. Below the upper depleted zone the centre core exhibits a gradual increase of susceptibility value with increasing depth. The base of this core is strongly enhanced relative to the lysimeter average. The core from the S. W. corner appears to show some similarities to the centre core. However, separating these two regions of positive susceptibility is a zone of well developed zone of negative susceptibility values.

From these descriptions it is apparent that the flow regime in the lower part of lysimeter C is quite different from that in

lysimeter A. There are many possible explanations of this feature, and with some knowledge of the relative geometry, and environmental history of these two lysimeters it is meaningless to speculate on the cause of this disparency.

## CONCLUSIONS

Like our previous study of cores from the ORF lysimeter, these six cores from lysimeters A and C located at CANMET also show statistically significant susceptibility difference values within the tailings. However, there seems to be little similarity in the distribution of susceptibility difference values in the CANMET and ORF lysimeters. Both of the CANMET lysimeters examined in this report show strongly depleted susceptibility values in the surface layers, and especially in the centre of the lysimeter. The ORF lysimeter with the exception of a very localised reduced susceptibility zone, showed for the most part strongly enhanced susceptibility values in the surface layers. CANMET lysimeter A shows a susceptibility enhanced zone just below the surface depleted zone. With increasing depth the susceptibility difference values diminish. A minor depleted zone follows. This part is somewhat reminiscent of the ORF lysimeter. Locally this also shows a gradual susceptibility decrease with increasing depth, followed by a minor susceptibility depleted zone. The lower portion of CANMET lysimeter C below the surface depleted zone does not appear to exhibit any overall systematic pattern(s).

It is anticipated that the reasons for the discrepancies between the patterns that are emerging for these various lysimeters may arise from factors such as; lysimeter geometry, tailings origin (detailed magnetic mineral species in original tailings, and tailings grain size distribution), environmental history (length of run duration, rain amount, sun amount, biological interaction etc.). Accepting all these variables magnetic susceptibility is still providing a rapid method for locating zones of oxide mineral depletion or enhancement.

W. A. Morris

TABLE 1

LYSIMETER A

| | N. W. CORNER | CENTRE | S. E. CORNER |
|---|---|---|---|
| 1 | -0.44 | -0.29 | -0.58 |
| 2 | -0.14 | -0.03 | -0.27 |
| 3 | -0.02 | +0.04 | +0.01 |
| 4 | +0.08 | +0.09 | +0.10 |
| 5 | +0.08 | +0.09 | +0.13 |
| 6 | +0.11 | +0.06 | +0.13 |
| 7 | +0.05 | +0.08 | +0.12 |
| 8 | +0.03 | +0.04 | +0.11 |
| 9 | +0.02 | -0.00 | +0.07 |
| 10 | +0.01 | +0.01 | +0.06 |
| 11 | -0.00 | +0.01 | +0.03 |
| 12 | +0.05 | -0.04 | +0.05 |
| 13 | +0.12 | -0.05 | +0.05 |

LYSIMETER LOG MEAN IS 13.7 $\times 10^{-6}$ emu.

Values quoted in tables are in $\log_{10}$ (deviation) from the

$\log_{10}$ (Lysimeter log mean $*10^{-6}$ )

TABLE 2

LYSIMETER C

| | N. E. CORNER | CENTRE | S. W. CORNER |
|---|---|---|---|
| 1 | -0.20 | -0.72 | -0.39 |
| 2 | +0.20 | -0.33 | -0.05 |
| 3 | +0.26 | -0.12 | +0.02 |
| 4 | +0.21 | -0.03 | +0.06 |
| 5 | +0.12 | +0.02 | +0.09 |
| 6 | +0.10 | +0.01 | -0.00 |
| 7 | +0.04 | +0.04 | -0.08 |
| 8 | -0.04 | +0.07 | -0.24 |
| 9 | +0.01 | +0.07 | -0.31 |
| 10 | -0.01 | +0.11 | -0.10 |
| 11 | -0.04 | +0.18 | +0.07 |
| 12 | +0.06 | +0.22 | +0.18 |
| 13 | +0.01 | +0.26 | +0.26 |

LYSIMETER LOG MEAN IS 16.4 $\times 10^{-6}$ emu.

Values quoted in tables are in $\log_{10}$ (deviation) from the $\log_{10}$ (Lysimeter log mean $*10^{+6}$)

LYSIMETER A

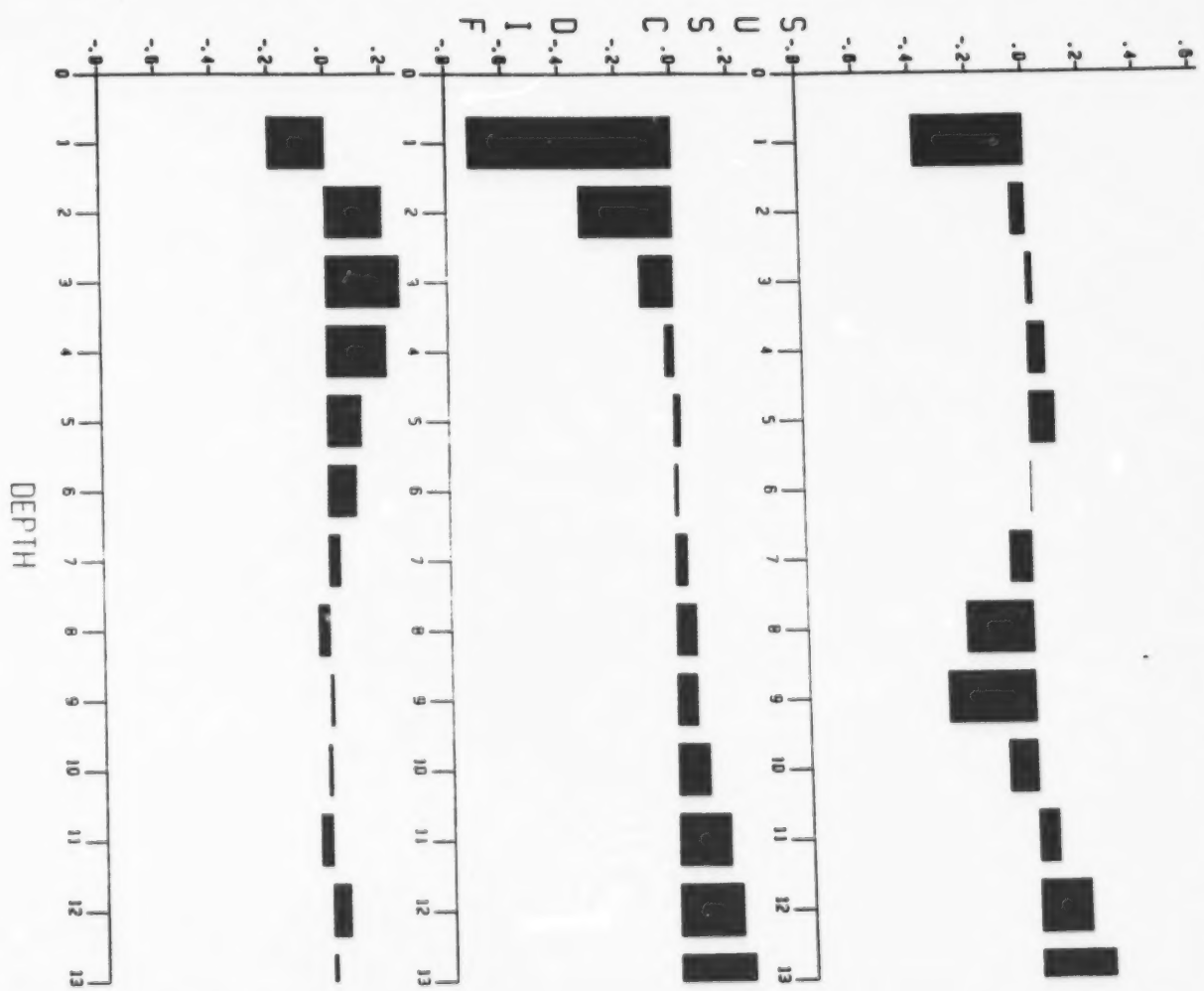


LYSIMETERC

TITLE

# MEASUREMENT OF MAGNETIC SUSCEPTIBILITY ON TAILINGS CORES

## REPORT ON CORES FROM CANMET LYSIMETERS

## LYTA B AND LYTA C

Work on this project was conducted under the auspices of the National Uranium Tailings Program of the Canada Centre for Mineral and Energy Technology, Energy, Mines and Resources Canada.

DSS FILE NO. 15SQ.23241-4-1648

DSS CONTRACT SERIAL No. OSQ84-00103

CANMET PROJECT NO.

CANMET SCIENTIFIC AUTHORITY: Mr. G. M. Ritcey

NOVEMBER 1984

## INTRODUCTION

Single cores from lysimeters, lyta B and lyta C located at the CANMET facilities in Ottawa have been examined for magnetic susceptibility variations with depth. All measurements were made on the full core enclosed in its ABS plastic container. Measurements were made using a Sapphire Instruments SI-1 susceptibility bridge with a 2.5 cm wide, and 7.5 cm diameter pass through coil. The same measurement procedures as used in the previous studies were retained in this study.

RESULTS

Table 1 and figures 1 and 2 present the details of the susceptibility difference values found in lysimeters Lyta B and Lyta C.

The log mean susceptibility values for respectively Lyta B and Lyta C are $16.67 \times 10^{-6}$ emu, and $20.56 \times 10^{-6}$ emu. Like the results from Ottawa lysimeters A and C there is a significant difference between the mean values for these two cores. Reasons for this discrepancy may include; a) different sources of the tailings in the two lysimeters; b) if of the same source then some separation may have occurred when the two lysimeters were constructed; and c) the discrepancy may reflect the total removal of some iron species from one lysimeter relative to the other.

Figure 1 and Table 1 present the data obtained for Lyta B. Like the other Ottawa lysimeters this shows a strongly susceptibility depleted surface zone. In this case the zone is over 15 cm thick, and the depletion reaches values of -0.4 log Susceptibility units. This surface zone is followed by an intermediate depth zone of average susceptibility values. A lower zone of approximately 12 cm thickness exhibits strongly enhanced susceptibility values.

In summary Lyta B exhibits surface depletion and basal enrichment of magnetic mineral species.

Figure 2 and Table 1 present the data obtained from Lyta C. Susceptibility variations along the length of this core are poorly developed and show little systematic pattern. The immediatly uppermost level is depleted, below this there is some localised enrichment. Depletion zones are also detected in the middle of the core, and also most surprisingly at the base of the core.

## CONCLUSIONS

These cores have more in common with the other Ottawa lysimeter A and C cores. All these cores show a susceptibility depleted surface zone. The depth extent and magnitude of this zone varies from core to core. Likewise many of these cores show locally enhanced basal zones. Both of these features are in direct contrast to the ORF results which are characterised by a surface enhanced susceptibility, and basal depleted susceptibility.

TABLE 1

SUSCEPTIBILITY DIFFERENCE VALUES FOR

LYTA B AND LYTA C

| | LYTA B | | LYTA C |
|---|---|---|---|
| 1 | -0.23 | 1 | -0.02 |
| 2 | -0.14 | 2 | +0.12 |
| 3 | -0.29 | 3 | +0.05 |
| 4 | -0.29 | 4 | +0.05 |
| 5 | -0.28 | 5 | +0.10 |
| 6 | -0.18 | 6 | +0.03 |
| 7 | -0.03 | 7 | -0.14 |
| 8 | +0.04 | 8 | -0.12 |
| 9 | +0.05 | 9 | +0.04 |
| 10 | +0.05 | 10 | +0.07 |
| 11 | -0.04 | 11 | +0.04 |
| 12 | +0.03 | 12 | -0.01 |
| 13 | +0.20 | 13 | -0.08 |
| 14 | +0.30 | 14 | -0.15 |
| 15 | +0.36 | | |
| 16 | +0.32 | | |
| 17 | +0.13 | | |

Log mean average for Lyta B is $1.667 \times 10^{-5}$ emu
root mean squared deviation is $8.154 \times 10^{-7}$

Log mean average for Lyta C is $2.056 \times 10^{-5}$ emu
root mean squared deviation is $7.105 \times 10^{-7}$

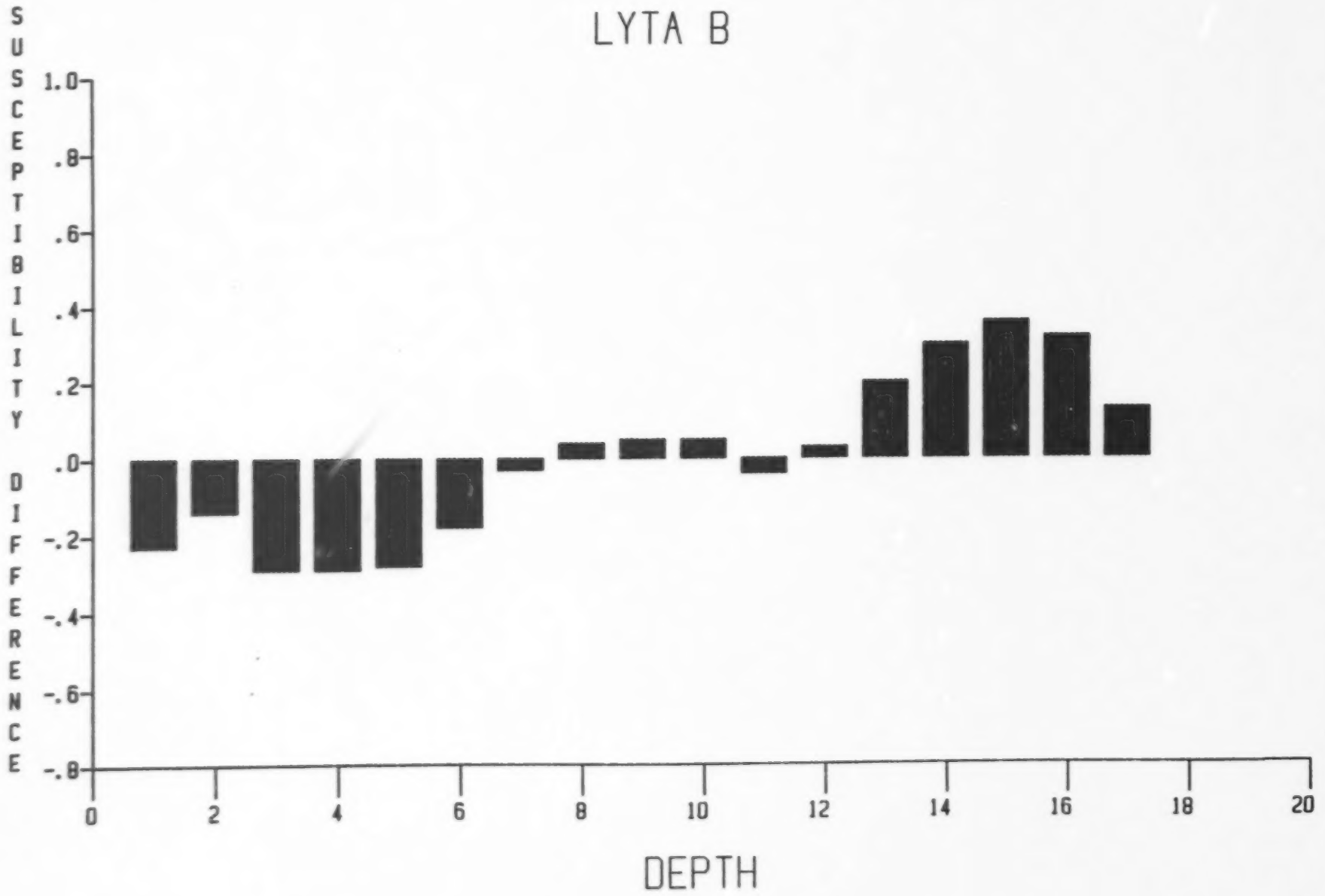
LYTA B
SUSCEPTIBILITY DIFFERENCE
1.0
.8
.6
.4
.2
.0
-.2
-.4
-.6
-.8
0
2
4
6
8
10
12
14
16
18
20
DEPTH

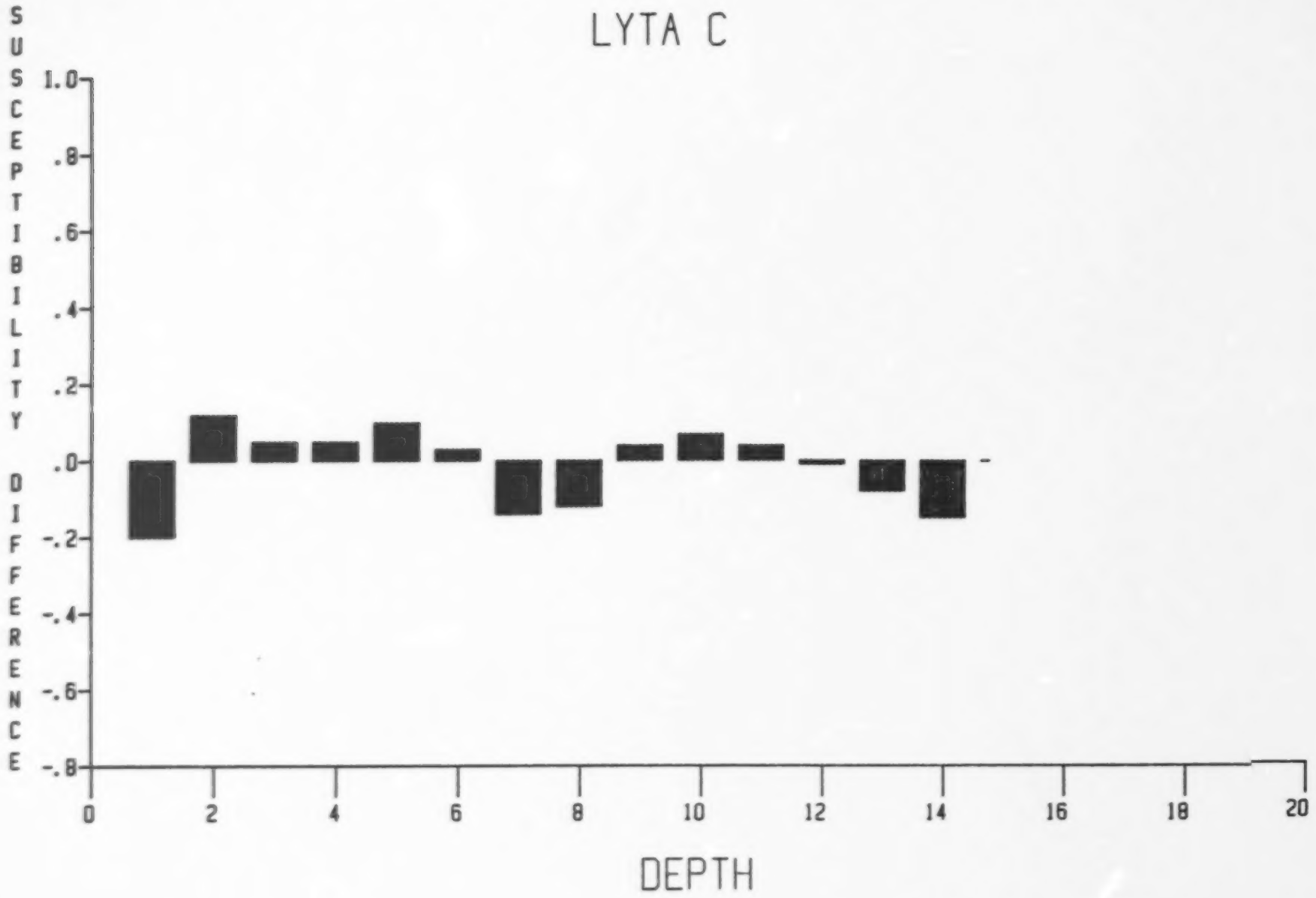
LYTA C
SUSCEPTIBILITY DIFFERENCE
1.0
.8
.6
.4
.2
.0
-.2
-.4
-.6
-.8
0
2
4
6
8
10
12
14
16
18
20
DEPTH

TITLE

MEASUREMENT OF MAGNETIC SUSCEPTIBILITY ON TAILINGS CORES

REVIEW

Work on this project was conducted under the auspicies of the National uranium Tailings Program of the Canada Centre for Mineral and Energy Technology, Energy, Mines and Resources, Canada.

DSS FILE No. 15SQ.23241-4-1648

DSS CONTRACT SERIAL No. 0SQ84-00103

CANMET PROJECT No.

CANMET SCIENTIFIC AUTHORITY: Mr. G. M. Ritcey

NOVEMBER 1984

REVIEW

The object of this contract was to examine the bulk magnetic susceptibility variations in uranium tailings which had been exposed to controlled environmental conditions. Two sets of uranium tailings type were examined. Cores obtained from the Ontario Research Foundation lysimeter located in Sheridan Park, Toronto contained tailings from the Athabasca Basin, Midwest Lake uranium camp. Typical of these tailings is the presence of arsenic, and nickel often associated with arsenopyrite. At the time of sampling the tailings pile had undergone four environmental campaigns; a) initial deposition Canada Wide Mines study, b) second deposition cycle, c) shutdown phase, d) examination of freezer and acidification of rain. Lithologically all these cores were of silt grain size showing very well developed horizontal layering. Near the surface the cores had a distinct red colouration, while at depth there was predominance of greys and yellows.

The second suite of cores were supplied from CANMET lysimeters located in Ottawa. It is my understanding that tailings in these lysimeters wre all obtained from the Elliot Lake uranium camp. Tailings from this area are typified by having a sand grain size, and containing free quartz and pyrite. Arsenopyrite is absent. All these cores show a rusty colouration, the intensity of the colouring varying along the length of the core. The environmental

history of these samples is unknown to this investigator.

Susceptibility measurements were all made using the Sapphire Instruments SI-1 susceptibility bridge. Measurements on the ORF tailings were made using a 7.0 cm wide, 7.5 cm diameter pass through coil. The CANMET tailings were measured using a 2.5 cm wide, 7.5 cm diameter pass through coil. Readings were taken at 2.5 interval along each core. Because of the difference of coil width data resolution is better for the CANMET tailings. The susceptibility variations in the tailings are represented by the $\log_{10}$ (susceptibility value) deviation from the $\log_{10}$ (average susceptibility value for the whole lysimeter).

The ORF tailings show three distinct zones of susceptibility character. The upper zone is dominated by strongly enhanced susceptibility values. Areas of susceptibility depletion are of limited extent and appear to define a direct run-off across the surface. In the intermediate zone there is an equal amount of susceptibility enhanced, and susceptibility depleted areas. The depleted zones define a dendritic drainage pattern all pointing towards the centre of the beach area on the downstream end of the tailings pile. With increasing depth in the tailings the susceptibility depleted areas become gradually more extensive. At the base of the tailings only locally restricted areas of susceptibility enhancement remain.

Figures 1, 2 and 3 compare the variation of uranium content on cores collected at the completion of campaign (solid lines) and the susceptibility difference variations (dashed lines) on our cores. Measurements of these two properties were not made on the same cores and the magnetic property data tells us that variations occur over relatively short distances. And different unit depth spacings were used on the two cores that were being compared. One therefore should not expect perfect correlation between the two properties. However, as shown by figures 1, 2 and 3 there is a broad similarity between the susceptibility difference and the uranium content. In most of the examples we have taken the inverse of the susceptibility data, suggesting an anti-correlation between oxide mineral concentration and uranium deposition.

In contrast most of the CANMET lysimeters which contain Elliot Lake tailings are characterised by susceptibility reduced values in the near surface zone and susceptibility enhanced values at the base of the lysimeter. Most often the intermediate depth zone is characterised by non-anomalous susceptibility values. No chemical data were supplied for this collection. Hence is is not possible to determine the relationship between uranium content and susceptibility for this collection.

SUMMARY

1) Statistically significant variations of bulk magnetic susceptibility can be detected both between, and along cores of uranium tailings obtained from lysimeter experiments.

2) Studies on cores from the Ontario Research Foundation lysimter experiment of Mid-West Mine, Athabasca Basin tailings indicate a broad anti-correlation exists between uranium content and susceptibility difference value.

3) The ORF tailings exhibit a simple threefold subdivision;

a) a surface zone of mainly enhanced susceptibility values, with very narrow localised zones of susceptibility depletion.

b) an intermediate zone with dendritic drainage pattern defined by regions of susceptibility depletion.

c) a basal zone of extensive susceptibility depletion. Areas of susceptibility enhancement only remain at the upstream limits of the bed.

4) The CANMET tailings also exhibit a threefold subdivision:

a) a surface depletion zone

b) an intermediate zone of non-anomalous values

c) a basal zone of enhanced susceptibility.

The correlation of these values to uranium content is unknown.

5) Clearly the magnetic method is capable of distinguishing some basic difference between the environmental evolution history of the Elliot Lake and Athabasca Basin tailings.

Whether this is a function of different environmental conditions of the lysimeters, or the pyrite/arsenopyrite contrast of the ore material remains to be analysed.

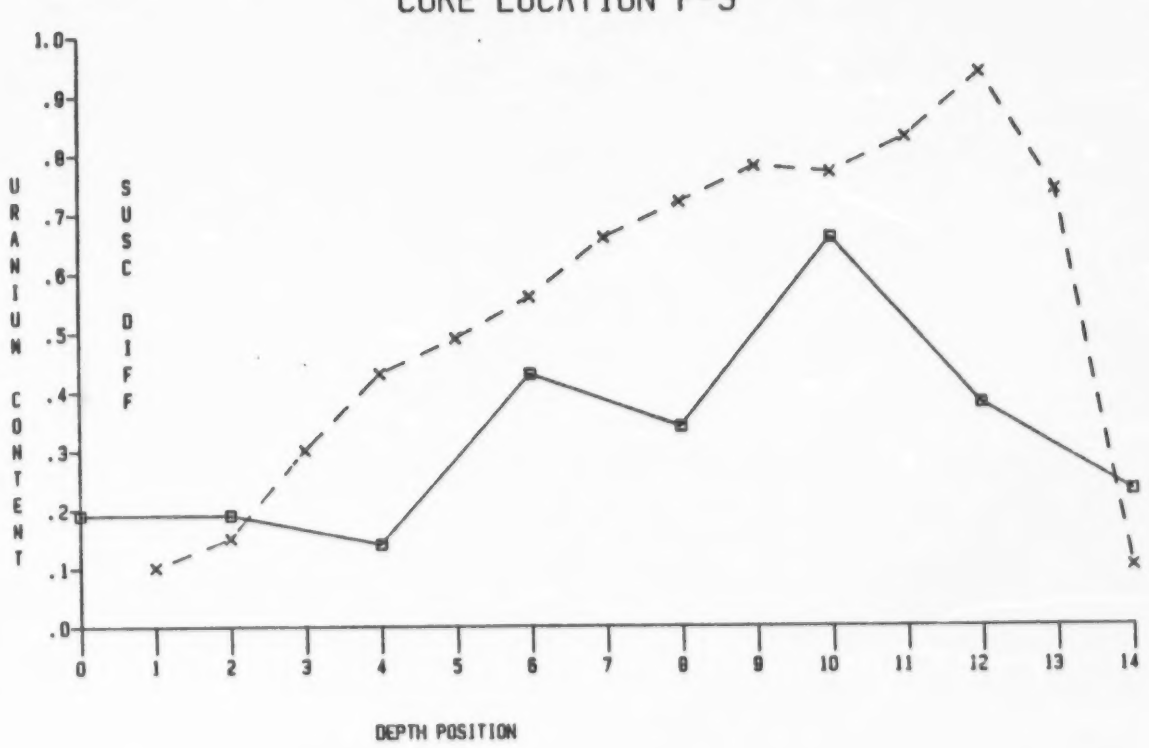
CORE LOCATION F-S
URANIUM CONTENT
SUSC DIFF
1.0
.9
.8
.7
.6
.5
.4
.3
.2
.1
.0
0 1 2 3 4 5 6 7 8 9 10 11 12 13 14
DEPTH POSITION

FIGURE 1

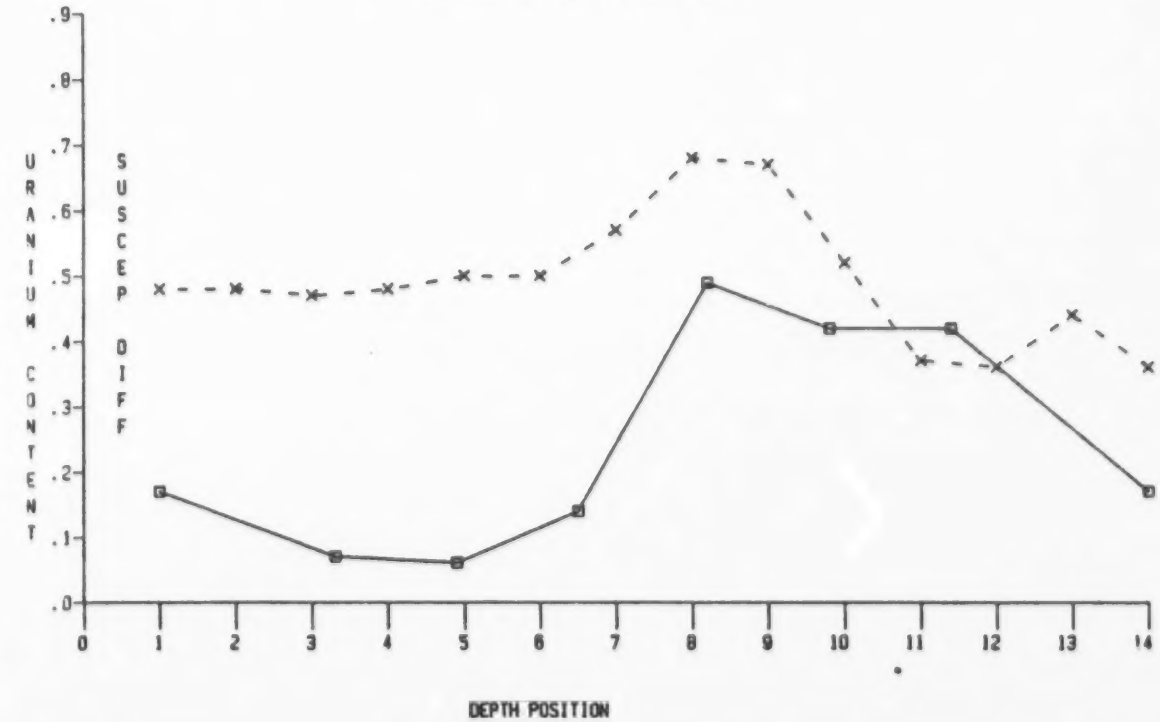
CORE LOCATION C-7
URANIUM CONTENT
SUSCEP DIFF
.9
.8
.7
.6
.5
.4
.3
.2
.1
.0
0 1 2 3 4 5 6 7 8 9 10 11 12 13 14
DEPTH POSITION

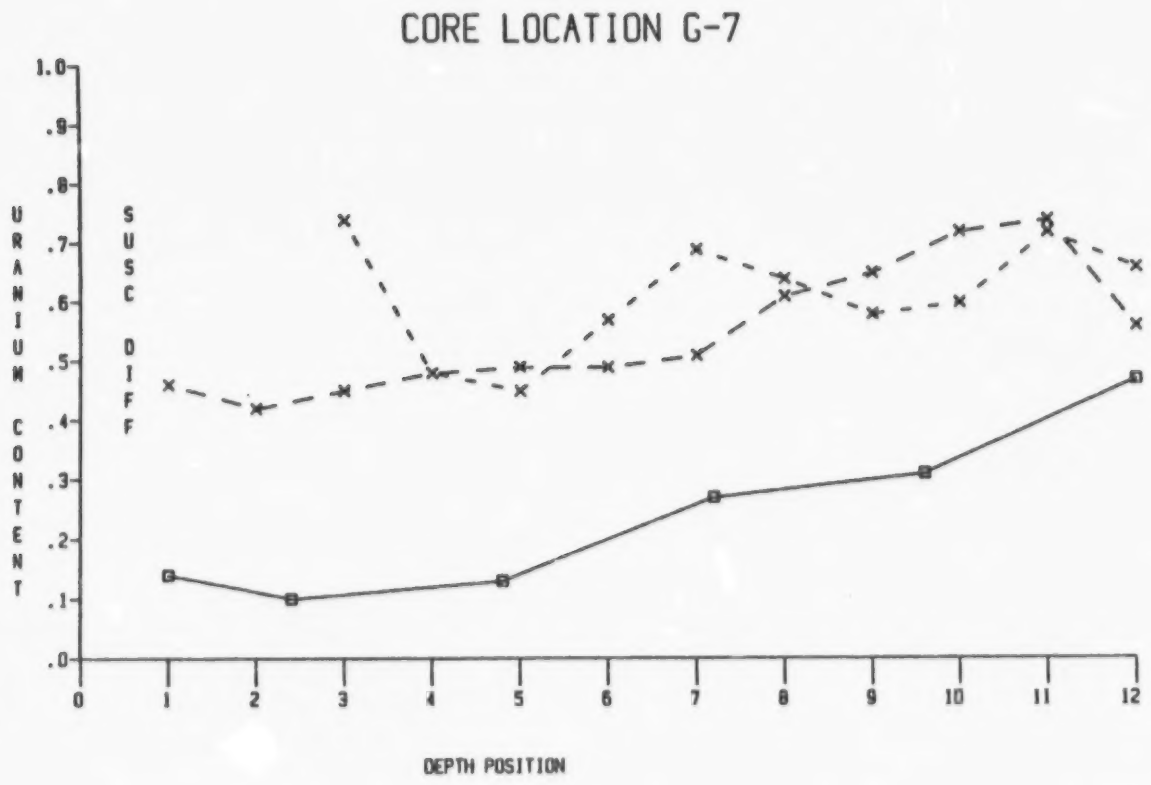
CORE LOCATION G-7
URANIUM CONTENT
SUSC DIFF
1.0
.9
.8
.7
.6
.5
.4
.3
.2
.1
.0
0
1
2
3
4
5
6
7
8
9
10
11
12
DEPTH POSITION

FIGURE 2

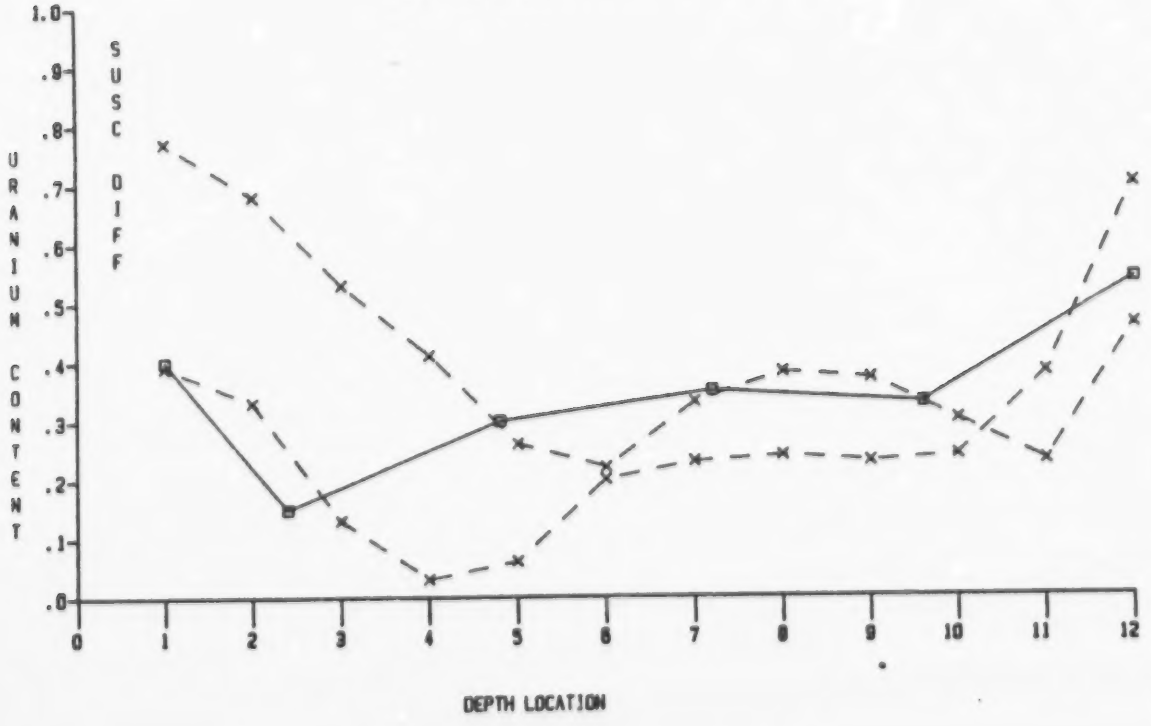
CORE LOCATION G-2
URANIUM CONTENT
SUSC DIFF
1.0
.9
.8
.7
.6
.5
.4
.3
.2
.1
.0
0
1
2
3
4
5
6
7
8
9
10
11
12
DEPTH LOCATION

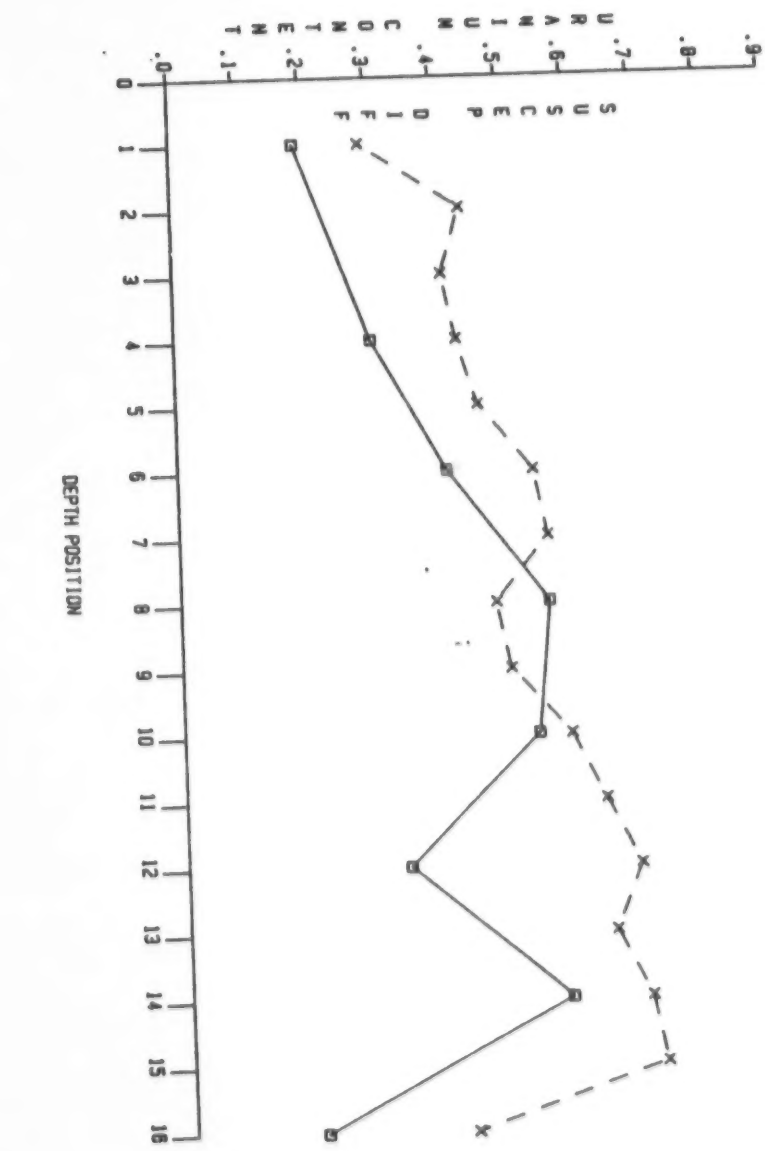
CORE LOCATION C-2
DEPTH POSITION
DIFF
SUSCEP
0
1
2
3
4
5
6
7
8
9
10
11
12
13
14
15
16
.0
.1
.2
.3
.4
.5
.6
.7
.8
.9

figure 3